The late Miocene Erinaceidae and Dimylidae (Eulipotyphla, Mammalia) from the Pannonian region, Slovakia

Florentin Cailleux, Lars W. van den Hoek Ostende and Peter Joniak

DOI:
http://dx.doi.org/10.1017/jpa.2023.50

Journal of Paleontology, 97(4), 2023, p. 777–798

Published by Cambridge University Press
on behalf of The Paleontological Society
0022-3360/23/1937-2337
doi: 10.1017/jpa.2023.50

JOURNAL OF PALEONTOLOGY
A PUBLICATION OF THE Paleontological SOCIETY

The late Miocene Erinaceidae and Dimylidae (Eulipotyphla, Mammalia) from the Pannonian region, Slovakia

Florentin Cailleux,[1,2]* Lars W. van den Hoek Ostende,[2] and Peter Joniak[1]

[1]Comenius University in Bratislava, Faculty of Natural Sciences, Department of Geology and Paleontology, Ilkovičova 6, Mlynská dolina G, SK–842 15 Bratislava, Slovakia <florentin.cailleux@naturalis.nl> <peter.joniak@uniba.sk>
[2]Naturalis Biodiversity Center, Darwinweg 2, 2333 CR Leiden, The Netherlands <lars.vandenhoekostende@naturalis.nl>

Non-technical Summary.—The late Miocene (11.5–5.5 million years ago) was a period of faunal change for small mammal communities. The evolution of several climatic parameters has greatly impacted faunas from Europe, and the surviving species also had to deal with the competitive pressure of new migrant species into Europe. In this context, mammal groups having high sensitivity to climatic parameters, such as temperature and humidity, show peculiar patterns of evolution. This is the case for the Erinaceidae (hedgehogs and gymnures) and the extinct family Dimylidae, well recorded in the fauna from the late Miocene of Slovakia. At least six Erinaceidae and two Dimylidae were present in Slovakia during that time, as shown by material extracted from the localities of Borský Svätý Jur, Krásno, Pezinok, Šalgovce, Studienka, and Triblavina. Both families were extremely abundant during the early part of the late Miocene, the Vallesian (11.5–9.0 million years ago), supporting the idea that central Europe played an important role in the preservation of high paleodiversity of insectivore species. However, the abundance of the Erinaceidae and Dimylidae strongly declined afterward, eventually leading to the extinction of the Dimylidae soon after the Vallesian. On a smaller scale, the material described from the late Miocene of Slovakia brings a lot of new information about the morphology, variability, and phylogeny of the identified species, namely '*Schizogalerix*' *voesendorfensis*, *Schizogalerix* cf. *S. moedlingensis*, *Lantanotherium sanmigueli*, *Atelerix* cf. *A. depereti*, *Atelerix* aff. *A. depereti*, cf. *Postpalerinaceus* sp. indet., Erinaceinae gen. indet. sp. indet., *Plesiodimylus chantrei*, and *Metacordylodon* aff. *M. schlosseri*.

Abstract.—The families Erinaceidae and Dimylidae are represented in the late Miocene localities of Slovakia (Borský Svätý Jur, Krásno, Pezinok, Šalgovce, Studienka, and Triblavina) by at least six hedgehog species—'*Schizogalerix*' *voesendorfensis* (Rabeder, 1973); *Schizogalerix* cf. *S. moedlingensis* (Rabeder, 1973); *Lantanotherium sanmigueli* Villalta and Crusafont, 1944; *Atelerix* cf. *A. depereti* Mein and Ginsburg, 2002; *Atelerix* aff. *A. depereti,* cf. *Postpalerinaceus* sp. indet., and Erinaceinae gen. indet. sp. indet.—and two dimylid species—*Plesiodimylus chantrei* Gaillard, 1897; and *Metacordylodon* aff. *M. schlosseri* (Andreae, 1904). Material of *L. sanmigueli* from the western Carpathians was investigated, revealing broad variability in all samples. Additionally, the deciduous premolars of *Lantanotherium* Filhol, 1888 are described here for the first time. Erinaceid species are frequent in the Vallesian but their abundance strongly declined afterward. As an exception, *Schizogalerix* Engesser, 1980 re-entered the Danube and Vienna basins during MN11, likely from eastern Europe. Members of Erinaceinae display low diversity during the late Miocene of central Europe, which tends to support a pan-European diversity phenomenon. The humidity-dependent Dimylidae spp. were abundant during the late Vallesian. Rare finds of *Plesiodimylus* Gaillard, 1897 confirm the survival of this family into the early MN11 in the Pannonian region.

Introduction

The Vallesian (11.2–9.9 Ma) represents a period of major faunal turnover among mammals (Agustí and Moyà-Solà, 1990; Van der Made et al., 2006; Daxner-Höck et al., 2016). Within the order Eulipotyphla, the decline of Aragonian (17.2–11.2 Ma) taxa was partially counterbalanced by migratory waves into Europe with the return of warmer and more humid environments (Furió and Agustí, 2017). These migrations had their origins in Anatolia and western to eastern Asia (Ziegler, 2006a; Van den Hoek Ostende et al., 2016; Cailleux et al., 2020). As a result, the Vallesian is characterized by high abundance of insectivore taxa in Europe (Furió et al., 2017) and the overall success of forest-adapted taxa. Notably, Eulipotyphla were especially diversified in central Europe (e.g., Van Dam, 2004; Van den Hoek Ostende et al., 2020), which is related to wetter environmental conditions (Furió et al., 2011b). However, the end of the Vallesian is characterized by a deterioration of these conditions, favored by the progressive settlement of seasonality (Van Dam, 2006).

From a biogeographical point of view, central Europe is a strategic area to study the record of newly arriving taxa and the pattern of faunal dynamics in Eulipotyphla during the

*Corresponding author.

Miocene because it constituted an important migration corridor. The evolution of Lake Pannon (Magyar et al., 1999) surely had an additional regional effect. Slovakia, strategically situated in the northern part of the Pannonian Basins System (PBS; Fig. 1), has preserved several vertebrate sites of major importance that help to understand the faunal evolution of central Europe, because it was affected during the late Miocene by uplift of the western Carpathians and the regression of the megalake (Joniak et al., 2020).

Recent excavations have yielded a series of late Miocene localities, testifying the rich micromammal record of the area (Fig. 1). The first results on the rodents of these localities have already been published (e.g., Joniak, 2005, 2016; Joniak and Šujan, 2020). However, whereas the late Miocene Eulipotyphla and Chiroptera from the Austrian part of the Danube and Vienna basins (northwestern part of the PBS; Fig. 1) have been fully described (e.g., Bachmayer and Wilson, 1970, 1978; Ziegler, 2006b, 2006a), no detailed work has been done on the Slovak material. As a first step toward understanding the late Miocene Eulipotyphla and Chiroptera from Slovakia, this work focuses on Erinaceidae and Dimylidae, two families frequently encountered in the early-late Miocene.

Geological setting

The Miocene sedimentary history of Slovakia is closely connected to the evolution of the western Carpathians and the Paratethys Sea. The sedimentary sequences of the large Danube Basin demonstrate well the coevolution of these structures (Kováč et al., 2017). The formation of the extensive Danube Basin began in the early Miocene with the stretching of the forearc basins at the western margin of the Carpathians. The Vienna Basin and the Slovak parts of the Danube Basin constituted the northwesternmost part of the PBS (Fig. 1) (Kováč et al., 2011), which was covered by a large lake system during the late Miocene (Harzhauser and Mandič, 2008; Kováč et al., 2011; Magyar et al., 2013). The PBS was still connected to the eastern Paratethys Sea during the early Sarmatian (ca. 13.5 Ma, according to Magyar et al., 1999) until the middle–late Miocene transition when Lake Pannon emerged (ca. 12 Ma according to Magyar et al., 1999; Joniak and Šujan, 2020). The progressive retreat of the Pannonian lake during the late Miocene (after ca. 9.5 Ma, according to Magyar et al., 1999) was characterized by the progradation of the paleo-Danube shelf margin from northwest to southeast, leading to the formation of a shift of different environments along Lake Pannon.

The large water mass of Lake Pannon reached its maximum extent in the early Vallesian, evidenced by the predeltaic deposits from Borský Svätý Jur (MN9) in the Slovak part of the Vienna Basin (Fig. 1) and by the slightly younger swamp deposits from Studienka (Sabol et al., 2021). These facies are grouped in the Ivanka Formation, ending with the retreat of Lake Pannon from the Danube Basin (Magyar et al., 2013).

The paleo-Danube River entered the PBS ca. 11–10 Ma from the western North Alpine Foreland Basin and initially went through the Vienna Basin (Šujan et al., 2016; Fig. 1). A new large deltaic structure in the northwestern part of the PBS was maintained by large water and sediment inputs from the paleo-Danube and other rivers. This period is represented in the Slovak Danube Basin by the Beladice Formation, containing the MN10 locality of Pezinok (Joniak, 2016; Fig. 1). At that time, the area was very humid, potentially due to orographic conditioned precipitation from the Alpine-Carpathian Arc (Utescher et al., 2017) and a system of shallow lakes and channels formed on the deltaic shelf. Consistently, the Beladice Formation is predominantly composed of coastal, lagoonal, and deltaic facies, ending with a heterogeneous southeastern progradation of the lake (Joniak and Šujan, 2020). This process was accompanied by the final decline of broadleaved evergreen vegetation in the northern part of the basin system (Utescher et al., 2017).

The deltaic phase was followed by the alluvial deposition of the Volkovce Formation in the study area. This phase is characterized by a noticeable spatial heterogeneity in deposits, which were strongly influenced by river dynamics and sediment supply. This is well-documented in sediments including the MN11 locality of Triblavina (Fig. 1) where the Volkovce Formation represent a transition from poorly drained to well-drained floodplains (Joniak and Šujan, 2020).

Krásno (Fig. 1), another MN11 small-mammal locality in Slovakia, yielded an abundant collection of material displaying a typical Turolian fauna. However, the depositional conditions in Krásno significantly differ from those in Triblavina. The fauna of Krásno was found within the Hlavina Member, which is characterized by the deposition of freshwater limestones alternating with calcareous silts and clays. Deposits of the Hlavina Member developed along active fault systems during uplift of the surrounding Carpathian massifs and continued at least until MN12, as documented by the fauna from Šalgovce (Sabol et al., 2021; Fig. 1), the youngest locality included in this work.

Materials and methods

The material described here comprises 264 isolated teeth of Erinaceidae and 110 isolated teeth of Dimylidae. For Erinaceidae, we mostly follow the measurement methods of Prieto and Rummel (2009), as shown in Figure 2, and the dental terminology of Klietmann et al. (2014a). Additionally, we use the term 'loph/lophid' to designate the fusion of two crests, and thus imply a clear and continuous connection between two cusps/cuspids. This includes the ectoloph (postparacrista + premetacrista), the paralophid (postparacristid + preprotocristid), and the protolophid (postprotocristid + premetacristid). Moreover, when the protoconule is distinguishable, the term 'preprotoconule crest' is used to indicate the crest labial of the cuspule.

We follow the measurement methods and dental terminology of Klietmann et al. (2014b) for Dimylidae (Fig. 3). The low bulge rarely observed near the paraconid is called 'accessory cuspid.'

All measurements are given in millimeters (mm). They were measured using a digital measuring microscope with a mechanical stage and digital measuring clocks. Full data (collection numbers, identifications, and specimen measurements) are provided in Supplementary Data Set 1. Specimens in figures are represented in left orientation; reversed specimens are

https://doi.org/10.1017/jpa.2023.50 Published online by Cambridge University Press

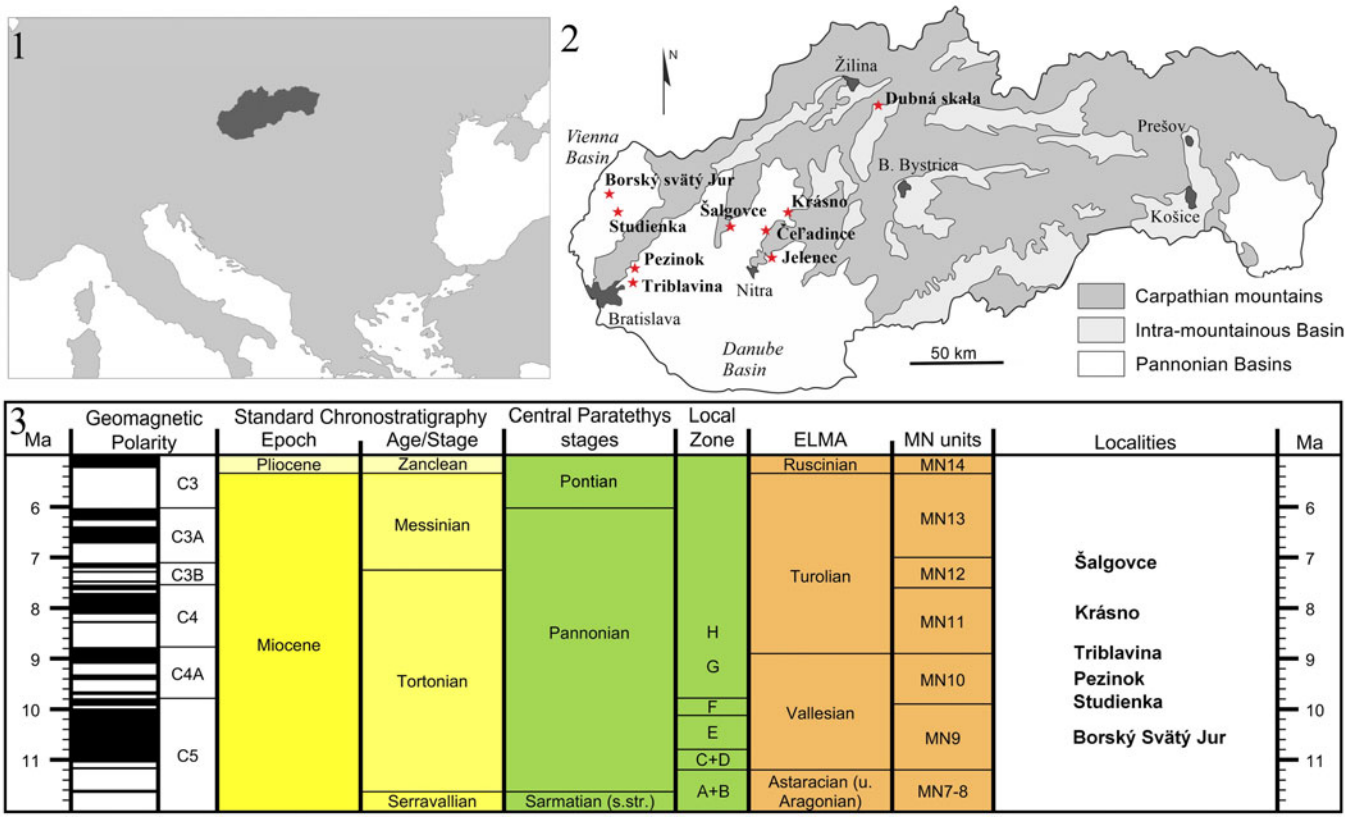

Figure 1. (**1**) Location of Slovakia within Europe. (**2**) Map of Slovakia showing the main geological structures and all of the late Miocene localities containing small mammals (red stars). (**3**) Preliminary stratigraphical correspondence of the localities studied in the present work (created with the software TimeScale Creator [v. 8.0, https://timescalecreator.org/]; MN units modified after Van Dam et al., 2023).

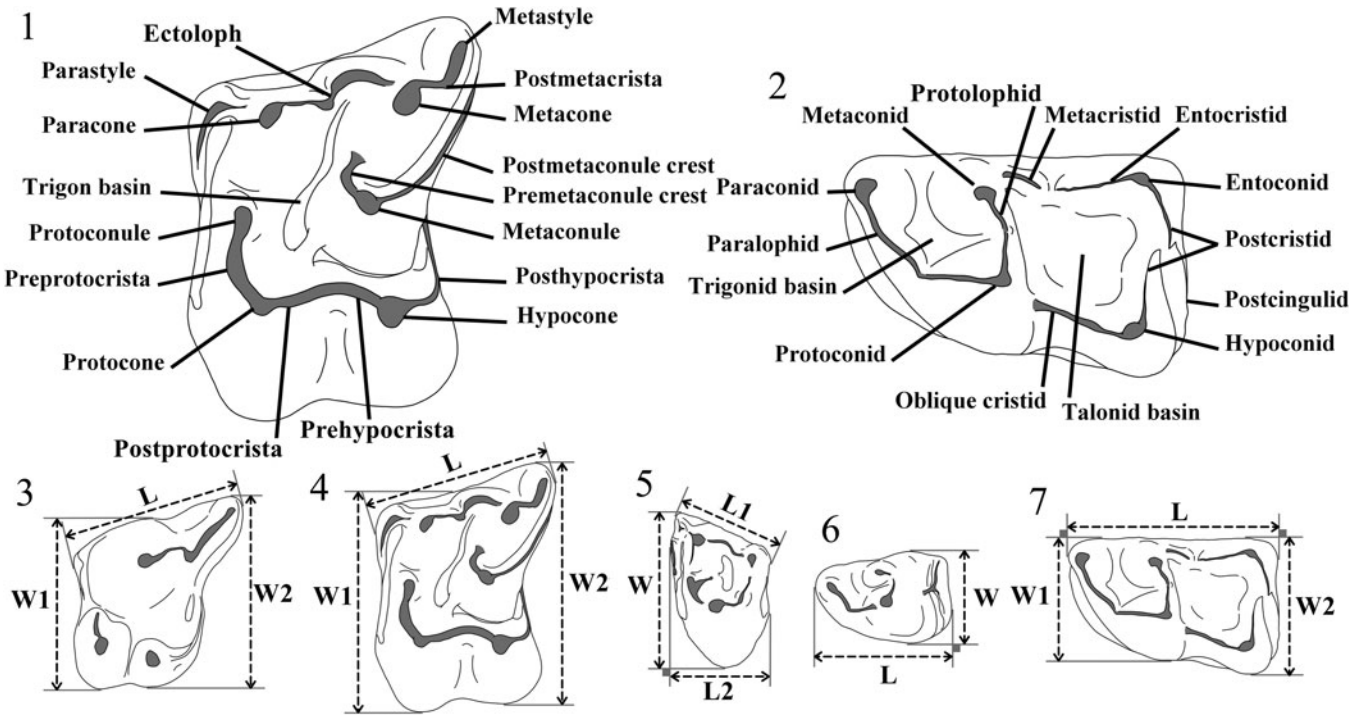

Figure 2. Terminology used for the M1 (**1**) and m1 (**2**) of Erinaceidae, and measurement protocols for P4 (**3**), M1 (**4**), M3 (**5**), p4 (**6**), and m1 (**7**). L = length; L1 = labial length; L2 = shortest anteroposterior length; W = width; W1 = anterior width; W2 = posterior width.

https://doi.org/10.1017/jpa.2023.50 Published online by Cambridge University Press

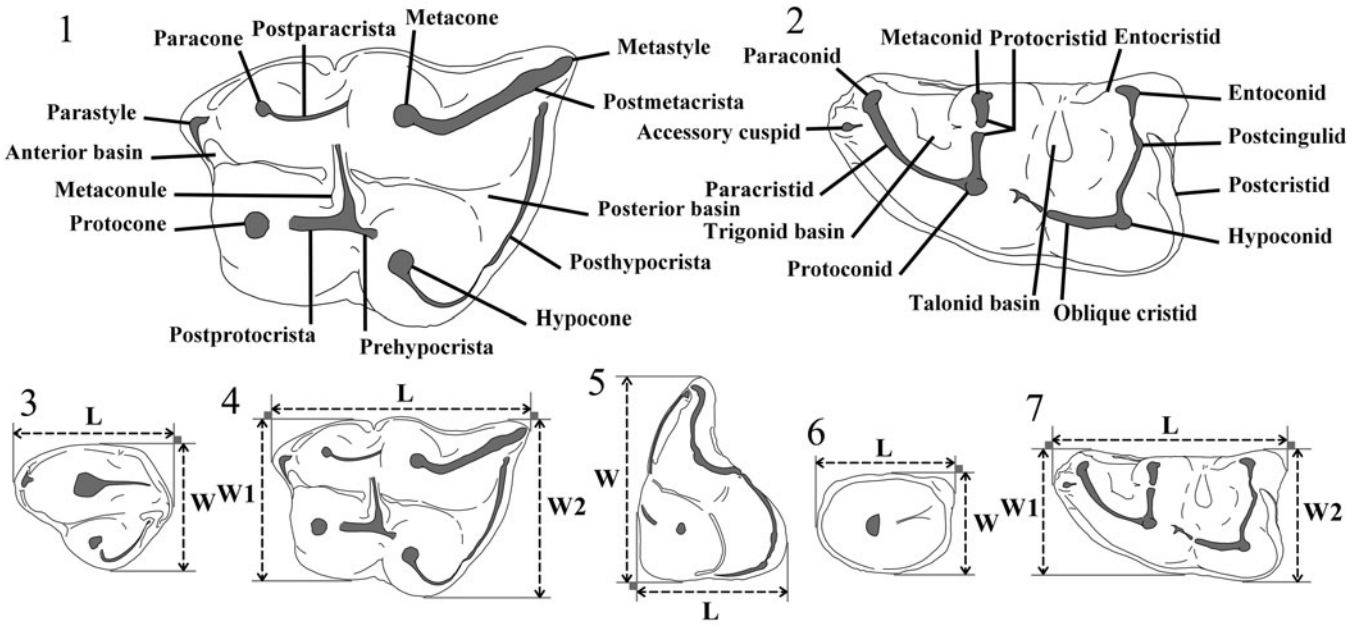

Figure 3. Terminology used for the M1 (**1**) and m1 (**2**) of Dimylidae, and measurement protocols for P4 (**3**), M1 (**4**), M3 (**5**), p4 (**6**), and m1 (**7**). L = length; W = width; W1 = anterior width; W2 = posterior width.

indicated by an underlined figure number. Unless otherwise noted, scanning electron micrographs (SEM) are shown in occlusal view. Drawings were obtained with a graphic tablet (Wacom Intuos Pro) and the software Autodesk SketchBook (v. 8.7.1, https://www.sketchbook.com). All of the described specimens are housed at the Department of Geology and Paleontology of Comenius University, Bratislava, Slovakia.

Abbreviations used in the text are: H = height; L = length; L1 = labial length; L2 = shortest anteroposterior length; N = number of specimens; W = width; W1 = anterior width; W2 = posterior width.

Repositories and institutional abbreviations.—ICP = Institut Català de Paleontologia Miquel Crusafont, Sabadell, Spain; MAFI = Hungarian Geological Institute, Budapest, Hungary; NHMA = Natural History Museum of Augsburg, Germany; NHMV = Natural History Museum of Vienna, Austria; UWPI = Institute of Paleontology, University of Vienna, Austria.

Systematic paleontology

Order Eulipotyphla Waddell, Okada, and Hasegawa, 1999
Family Erinaceidae Fischer, 1814
Subfamily Galericinae Pomel, 1848
Tribe Galericini Pomel, 1848
Genus *Schizogalerix* Engesser, 1980

Type species.—*Schizogalerix anatolica* Engesser, 1980.

Other species.—*Schizogalerix zapfei* (Bachmayer and Wilson, 1970); *S. moedlingensis* (Rabeder, 1973); '*S.*' *voesendorfensis* (Rabeder, 1973); *S. pasalarensis* Engesser, 1980; *S. samartica* (Lungu, 1981); *S. sinapensis* Sen, 1990; *S. macedonica* Doukas in Doukas et al., 1995; *S. duolebulejinensis* Bi et al., 1999; *S. intermedia* Selänne, 2003; and *S. evae* De Bruijn et al., 2006.

Diagnosis.—See Van den Hoek Ostende (2001, p. 686).

Occurrence.—Early–late Miocene of Anatolia (Sen, 1990; De Bruijn et al., 2006) and Asia (Bi et al., 1999; Zijlstra and Flynn, 2015); middle–late Miocene of Africa (Engesser, 1980; Cailleux, 2021); late-middle and late Miocene of Europe (Bachmayer and Wilson, 1970; Rabeder, 1973; Mein, 1999; Ziegler, 2006a).

Remarks.—The generic attribution of '*Schizogalerix*' *voesendorfensis* is put in quotation marks considering the strong similarities found between this species and representatives of *Parasorex* Meyer, 1865, especially *Parasorex socialis* Meyer, 1865, as already mentioned by Prieto et al. (2014) and Van den Hoek Ostende et al. (2016).

'Schizogalerix' voesendorfensis (Rabeder, 1973)
Figure 4.1–4.22; Table 1

Holotype.—Left M2, UWPI 1909/2/12.

Diagnosis.—See Prieto et al. (2010, p. 108).

Occurrence.—Late-middle to early-late Miocene (MN7+8, MN9) of central and western Europe (Rabeder, 1973; Ziegler, 2000; Prieto et al., 2010, 2014; Hír et al., 2016, 2017). The type locality is Vösendorf, Austria (MN9).

Description.—The upper canine has two compressed roots and simple morphology. The main cusp is situated slightly anteriorly. There is no posterior shoulder. The P1 is a highly

https://doi.org/10.1017/jpa.2023.50 Published online by Cambridge University Press

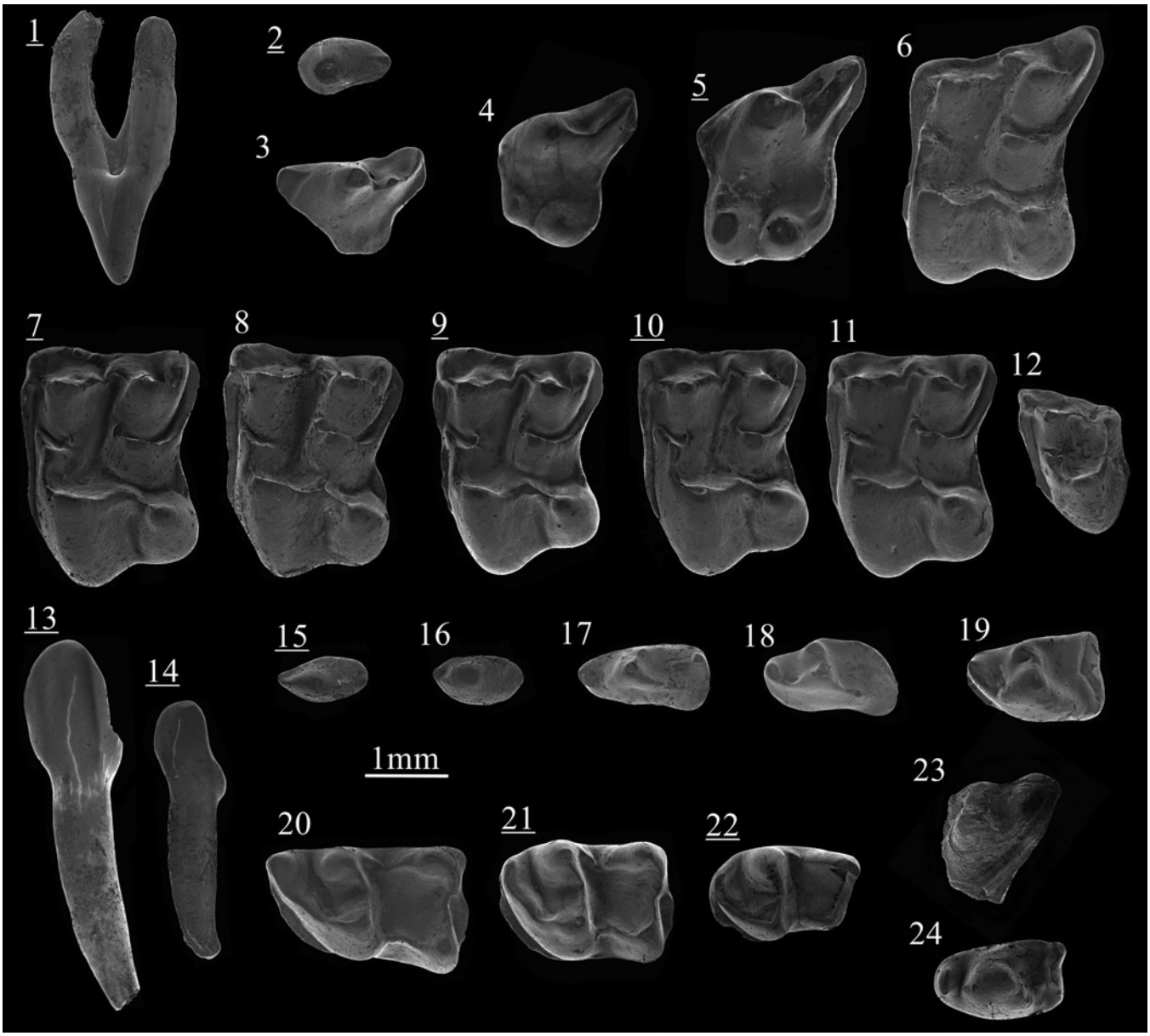

Figure 4. Scanning electron photomicrographs of '*Schizogalerix*' *voesendorfensis* (Rabeder, 1973) from Borský Svätý Jur (**1–22**) and *Schizogalerix* cf. *S. moedlingensis* (Rabeder, 1973) from Krásno (**23, 24**): (**1**) C, BJ213053, labial view; (**2**) P2, BJ213057; (**3**) dP3, BJ213180; (**4**) P3, BJ213172; (**5**) P4, BJ213071; (**6**) M1, BJ213014; (**7**) M2, BJ213029; (**8**) M2, BJ213033; (**9**) M2, BJ213035; (**10**) M2, BJ213045; (**11**) M2, BJ213047; (**12**) M3, BJ213075; (**13**) i1/2, BJ213133, labial view; (**14**) i3, BJ213029, labial view; (**15**) p1, BJ213063; (**16**) p2, BJ213061; (**17**) dp3, BJ213083; (**18**) dp4, BJ213092; (**19**) p4, BJ213091; (**20**) m1, BJ213140; (**21**) m2, BJ213154; (**22**) m3, BJ213158; (**23**) M1, KR127020; (**24**) p3, KR127028. Images with underlined numbers are reversed.

reduced tooth with no cingulum and a single bent cusp. The P2 has similar dimensions as the upper canine but has a less-sharp profile and an extended posterior bulge. An anteroposterior crest is present. The P3 is rounded and molarized. The postparacrista is a strong and moderately curved crest in which the metacone is included. This crest descends from the paracone with an anteroposterior orientation but ends at the posterolabial border of the tooth with an oblique orientation. The paracone is massive. There is no parastyle. The protocone is at the anterolingual border of the tooth and is situated more labial than the hypocone. The high protocone is somewhat compressed anteroposteriorly. The two lingual cusps are separated by a narrow valley. A hardly distinguishable crest starts from the low hypocone and leads to a cingulum running all along the posterior border. The dP3 is a subtriangular element with a paracone carrying a low posterior crest. The metacone and the metastyle are well differentiated. The parastyle is low and elongated. The lingual flange bears only a thin crest starting from the base of the paracone and ending as a minute bulge (protocone; see Fig. 4.3). The P4 is a solid premolar with a slight transverse elongation. The paracone is high and conical. A short parastyle is attached at its anterior base. The posterocrista is a large, short, bipartitioned crest. The postparacrista and premetacrista are merged into a single ridge (ectoloph) displaying an oblique orientation, creating an S-shaped labial margin. The metacone is usually absent

https://doi.org/10.1017/jpa.2023.50 Published online by Cambridge University Press

Table 1. Measurements (in mm) of '*Schizogalerix*' *voesendorfensis* (Rabeder, 1973) from Borský Svätý Jur, Slovakia. L = length; L1 = labial length; L2 = shortest anteroposterior length; W = width; W1 = anterior width; W2 = posterior width.

	C		P1		P2		DP3		P3			P4			M1		
	L	W	L	W	L	W	L	W	L	W1	W2	L	W1	W2	L	W1	W2
N	1	1	1	1	6	6	3	3	13	11	11	9	8	8	7	11	6
Min	-	-	-	-	1.08	0.65	1.60	0.90	1.65	1.31	1.56	2.05	2.01	2.26	2.28	2.51	2.94
Max	-	-	-	-	1.16	0.71	1.81	1.13	1.88	1.61	2.14	2.22	2.17	2.50	2.49	2.81	3.13
Mean	1.15	0.61	0.80	0.55	1.13	0.68	1.73	1.05	1.80	1.47	1.84	2.17	2.10	2.37	2.39	2.67	3.02
	M2			M3			i1		i2			p1		p2		dp3	
	L	W1	W2	L1	L2	W	L	W	L	W		L	W	L	W	L	W
N	18	20	17	9	8	8	2	2	4	4		1	1	7	7	2	2
Min	1.80	2.45	2.10	1.16	1.06	1.70	1.11	0.79	0.91	0.56		-	-	1.09	0.60	1.47	0.80
Max	2.09	2.81	2.33	1.42	1.23	1.94	1.14	0.84	0.98	0.65		-	-	1.18	0.72	1.59	0.81
Mean	1.95	2.65	2.55	1.28	1.14	1.81	1.13	0.81	0.95	0.61		1.07	0.53	1.12	0.64	1.53	0.81
	p3		dp4		p4		m1			m2			m3				
	L	W	L	W	L	W	L	W1	W2	L	W1	W2	L	W1	W2		
N	12	12	1	1	8	8	7	11	12	11	12	16	2	9	4		
Min	1.35	0.85	-	-	1.69	1.12	2.48	1.41	1.62	2.00	1.40	1.42	1.80	1.13	1.07		
Max	1.69	1.00	-	-	1.89	1.24	2.84	1.55	1.90	2.33	1.59	1.66	1.84	1.29	1.13		
Mean	1.50	0.92	1.69	0.85	1.77	1.17	2.64	1.49	1.72	2.04	1.49	1.54	1.82	1.19	1.09		

(Fig. 4.5); in one specimen, a metacone is distinguishable, creating a slightly stronger carnassial notch. The protocone is an anteroposteriorly compressed cusp, reaching half the height of the paracone. The preprotocrista starts from the anterior side of the protocone and runs on the anterior border until the middle part of the tooth; it is not connected to the parastyle area. The conical hypocone is lower than the protocone. A wide posterior cingulum starts from the hypocone, reaches the posterolabial margin, and closes the posterolingual basin.

The M1 is a quadrangular molar with no oblique elongation. The metacone is a conical cusp higher than the paracone. From its posterior border runs a high and curved metastyle. The S-shaped ectoloph starts from the labial side of the metacone. It is usually complete (N = 11) but is sometimes divided (N = 5; Fig. 4.6). The paracone is subtriangular and always connected to a well-developed parastyle by a thin ridge. The preprotocrista of the protocone is large and always bears a robust protoconule that has a variable base depending on the division of the preprotoconule crest: usually triangular, sometimes circular. The preprotoconule crest is always interrupted by a notch. The protocone is connected to the lower, conical hypocone by a curved crest. The posthypocrista joins the posterior cingulum in 13 of 15 specimens. There is no clear protocone-metaconule connection. The crescentic metaconule is situated in a more anterior position than the metacone and the hypocone. The postmetaconule crest is well developed and connected to the labial part of the postcingulum, isolating it from the shorter lingual part. The premetaconule crest ends at the base of the metacone. A continuous anterior cingulum joins the parastyle. The labial cingulum is always discontinuous.

The M2 has an anterior side wider than the posterior side. The metacone is compressed labial-lingually and the metastyle is shorter and more angular than in M1. The ectoloph is always S-shaped (N = 13; Fig. 4.7–4.11). The parastyle is strong and always connected to the conical paracone (N = 18). The protoconule is strong and the preprotoconule is often divided (nine of 15 specimens). In one molar, the anterior branch of the preprotoconule is connected to the anterior cingulum. The protocone is the strongest cusp, connected to the hypocone by a reverse V-shaped crest. There is no posthypocrista. One of 20 specimens (Fig. 4.8) shows a clear protocone-metaconule connection. The postmetaconule-postcingulum connection is always present, separating the postcingulum into two parts.

The M3 is a small subtriangular tooth showing anteroposterior compression. The triangular paracone is higher than the conical metacone; they are connected by an irregular ectoloph. An elongated parastyle is connected to the base of the paracone. The protocone is the highest cusp. The protocone-metacone connection is continuous whereas the protocone-paracone connection is interrupted by a notch at the base of the paracone. The protoconule is usually not visible. A continuous anterior cingulum joins the parastyle. The posterior cingulum, when present, forms a short median extension (Fig. 4.12).

An edentulous fragment of a mandible has been found, preserving the alveola of m2 and m3, and a part of the ascending ramus. The main characteristics are the small size of the m3 alveoli compared to those of m2, the circular anterior and elliptical posterior alveola of m3, the constricted posterior part of the corpus mandibulae, and the strong ramus.

The i1 is spatulate and asymmetrical. The crown is slightly projected forward, following the curve of the compressed root. The anterior base of the crown is concave whereas the posterior base has a short and low distal shoulder. The i2 is a smaller tooth reaching half the height of i1. The crown is more projected, the mesial concavity fitting with the distal shoulder of the anterior tooth. In three of four specimens, a median furrow is found in the lingual face of the compressed root.

The p1 is a simple monocuspid tooth with an enlarged root in which a median furrow can be distinguished. The only cusp is narrow and in an anterior position. A small bulge is present at the posterior end of the tooth, separated from the cusp by a shallow slope. The p2 is an elliptical two-rooted tooth bearing one circular to subtriangular main cusp in an anterior position. An anterolingual bulge is present; a larger bulge is found at the posterior border of the premolar. The dp3 is a narrow tooth characterized by a low and isolated paraconid. The protoconid is subtriangular with a convex lingual flank. The posterior margin is the broadest part of the tooth. The thin posterior cingulid bears

https://doi.org/10.1017/jpa.2023.50 Published online by Cambridge University Press

a cuspule. The p3 is a robust, double-rooted premolar with a low, usually independent paraconid. A curved paralophid is sometimes present, connecting the paraconid to the protoconid. The strong main cusp is flattened on its posterior side. A marked cingulid is present along its posterior margin. Rarely, a thin median crest is connected to the postcingulid. The dp4 presents the usual oblique elongation of Galericini. The paraconid is low and the paralophid short. The protoconid has an irregular outline. On its anterolingual side, a well-developed metaconid is attached, almost reaching the height of the protoconid. The posterior area is stretched: the labial part is longer than the lingual one (see Fig. 4.18). The postcingulid is curved. The p4 is a subtriangular tooth with two roots. The paraconid is included in a blade-like paralophid, separated from the triangular protoconid by a small notch. The metaconid is situated more anteriorly than the protoconid and reaches two-thirds its height. The posterior margin has a marked cingulid, higher in its median part. This creates a short basin open on the lingual and labial sides. There is a short anterolabial cingulid below the paralophid. In one of nine specimens, a cingulid is found between the paraconid and the metaconid.

The trigonid of the m1 is of similar length as the talonid. The paraconid is conical and connected to a subtriangular protoconid by a curved paralophid. The metaconid is situated more anteriorly than the protoconid. The trigonid basin is simple and narrow. The talonid area is characterized by two subtriangular cuspids. The entoconid is higher than the hypoconid. A high entocristid occupies the posterolingual border. The notch between the short metacristid and the entocristid is weak. The hypoconid is connected to the trigonid wall by an almost straight oblique cristid. The postcristid runs from the hypoconid, usually ending at the base of the entoconid or rarely reaching the posterior side of that cuspid. The posterior cingulid is strong and always connected to the entoconid, although it sometimes joins the postcristid before reaching the cusp. An anterolabial cingulid is always present, and rarely also a short ectocingulid.

The m2 differs from the m1 by its dimensions and more compressed trigonid (compare Fig. 4.20, 4.21). The paraconid is not differentiable from the curved and low paralophid. The subtriangular protoconid and the conical metaconid are of similar size. The talonid is somewhat longer than the trigonid. The entoconid is elongated and the entocristid high. The entoconid-metaconid connection is interrupted by a stronger notch than in the m1. The hypoconid is subtriangular, lower than the entoconid, and connected to the trigonid wall by a thin oblique cristid. The posterior cingulid is isolated (N = 2) or connected to the entoconid (N = 4). When connected, the posterior cingulid is fused with the curved postcristid. A narrow anterolabial cingulum is present. The ectocingulid is usually lacking, but one specimen bears a minute extension.

The m3 is a small two-rooted molar in which the trigonid is shorter than the talonid. The paraconid is included in the low curved paralophid. The conical metaconid is higher and situated in a more anterior position than the subtriangular protoconid. A strong elongated entoconid dominates the talonid. The metaconid-entoconid connection is weak but not interrupted. The short hypoconid is subtriangular and connected to the entoconid by a hardly distinguishable straight ridge. The anterolabial cingulid is present, but not the posterior one.

Materials.—Borský Svätý Jur: one C, one P1, six P2, 13 P3, three dP3, 16 P4, 23 M1, 26 M2, 11 M3, two i1, four i2, one p1, eight p2, two dp3, 13 p3, two dp4, nine p4, 20 m1, 24 m2, 12 m3, one fragment of mandible. See Table 1 for measurements.

Remarks.—*Schizogalerix* is a frequent member of late Miocene faunas in central Europe. Restricted to Anatolia during the early and most of the middle Miocene (Engesser, 1980; De Bruijn et al., 2006), a European group emerged during the late-middle Miocene including several species: '*Schizogalerix*' *voesendorfensis* (MN8, MN9), *S. sarmatica* (MN9), *S. moedligensis* (MN11, MN12), *S. zapfei* (MN10–MN12), and *S. macedonica* (MN13). A trend is observed through time with the progressive oblique elongation of P4 and upper molars, the division of the ectoloph, the complexification of M3, and the strength of the postcingulid-entoconid connection on the lower molars. It is worth noting that this group is not constituted by one lineage. The species from Borský Svätý Jur corresponds to the most basal morphological stage of this European group and displays all of the diagnostic features of '*S.*' *voesendorfensis*. This species was first recorded in the Hungarian locality of Felsőtárkány 2/3 ca. 12.1 Ma (see Hír et al., 2016) before its occurrences in the German locality of Gratkorn, ca. 12 Ma (see Prieto et al., 2010). Borský Svätý Jur and Vösendorf represent the last occurrences of this basal *Schizogalerix* in central Europe. The material from Borský Svätý Jur is morphologically more advanced than the late-middle Miocene occurrences. We found a very similar form in the Spanish locality of Nombrevilla 2, dated 11.9 Ma. Much of the Spanish Vallesian and Turolian material has been identified as *Parasorex ibericus* (Mein and Martín-Suárez, 1993). The relationship between '*S.*' *voesendorfensis* and the Iberian species needs to be illuminated, also to decide whether the central European species is best classified as a primitive *Schizogalerix* or rather indicates convergent evolution by an advanced species of *Parasorex*. In this respect, it is noteworthy, as Prieto et al. (2010) already observed, that there is a distinct morphological gap between '*S.*' *voesendorfensis* and *S. moedligensis*, especially in the upper molars.

Schizogalerix cf. *S. moedlingensis* (Rabeder, 1973)
Figure 4.23, 4.24

Diagnosis.—See Rabeder (1973, p. 433).

Occurrence.—*Schizogalerix moedlingensis* is known from its type locality, Eichkogel (MN11, Austria), and has been identified in Turolian localities from Greece, namely Pikermi and Pikermi-Chomateri (Doukas et al., 1995; Vasileiadou and Doukas, 2021).

Description.—The two labial fragments of P3 have a robust shape. The paracone is conical. From it descends a low and slightly curved metastyle reaching the posterior cingulum at the posterolabial margin of the tooth. There is no distinct parastyle, although a short anterolabial cingulum is present. The labial outline of the P4 is slightly curved. The paracone is conical and connected to a strong bipartitioned metastyle

https://doi.org/10.1017/jpa.2023.50 Published online by Cambridge University Press

ending in a more labial position than the paracone. The parastyle is well differentiated and is connected to both the base of the paracone and the anterior cingulum. The protocone is low and the hypocone well developed. Both cusps have a slight posterolabial orientation. A short and small crest running transversely from the protocone is distinguishable. Thin ridges are found between the two cusps and on both anterior and posterior margins.

The M1 is only represented by two fragments. The posterolabial fragment preserves a conical metacone connected to a metastyle by a short and curved crest. The anterior mesoloph is short and has a clear labial orientation (Fig. 4.23). A postmetaconule crest is present, but the metaconule is not preserved. The labial outline is curved with a median constriction. The second fragment corresponds to a protocone, a distinct protoconule, and a narrow anterior cingulum. A fragment of the triangular M3 shows a small and conical protocone connected to the base of a higher metacone by a low crest. A much lower crest is also distinguishable on the anterior margin of the molar. The paracone is missing in this specimen.

The p3 is a two-rooted tooth with an isolated, low, and pointed paraconid. The protoconid is conical and positioned in the middle of the tooth. Its posterior flank is slightly concave. The talonid consists mostly of a robust postcristid and a faint transverse ridge.

The trigonid and the talonid on m3 are of similar size. The paraconid is not distinguishable from the curved and low paralophid. The protoconid and metaconid are conical and connected by a thin but complete ridge. The trigonid basin is broad but shallow. The entoconid is strong and distinguishable from the high entocristid. The hypoconid is low. The postcingulid is well developed and connected to the entoconid. Only a slight ridge connects the two parts of the S-shaped postcristid.

Materials.—Krásno: two fragments of P3 (L = 1.78, 1.79), three fragments of P4 (L = 2.22, 2.28, third too fragmented to measure), two fragments of M1, one fragment of M3, one p3 (L = 1.63, W = 0.94), one m3 (L = 1.91, W1 = 1.27, W2 = 1.16).

Remarks.—The split ectoloph on the upper molars and the advanced development of the entoconid and postcingulid on the lower molars are significant features of *Schizogalerix*. The *Schizogalerix* from Krásno can be easily distinguished from the Moldovan *S. sarmatica* (MN9) by the much less oblique elongation of the P4. The derived stage of the ectoloph on M1 also excludes '*S.*' *voesendorfensis*. Two species have been identified in MN11 of central Europe: *S. zapfei* and *S. moedlingensis*, both being recorded in Austria (Rabeder, 1973; Ziegler, 2006a). *Schizogalerix zapfei* and *S. moedligensis* share a similar dental pattern that can make their identification difficult based on scanty material. Nevertheless, based on the material from Kohfidisch, we noticed a more complex ectoloph morphology in *S. zapfei*, whereas *S. moedlingensis* has more reduced mesostyles. The labial margin of the metacone area is always fully convex in *S. zapfei,* but is more irregular in *S. moedlingensis*, as in our specimen. The m3 of *S. zapfei* shows a distinct transverse pattern with a straight, oblique paralophid and a well-developed entoconid-postcingulid connection. This is not found in our specimen, in which the paralophid is clearly curved and the postcristid not fully divided, as in *S. moedlingensis*. In view of the limited material from Krásno, we classify the galericine as *S.* cf. *S. moedlingensis.*

Tribe Incertae sedis
Genus *Lantanotherium* Filhol, 1888

Type species.—*Erinaceus sansaniensis* Lartet, 1851.

Other species.—*Lantanotherium robustum* (Viret, 1940); *L. sanmigueli* Villalta and Crusafont, 1944; *L. longirostre* Thenius, 1949; *L. sawini* (James, 1963); *L. dehmi* (James, 1963); *L. lactorense* (Baudelot and Crouzel, 1976); *L. sabinae* (Mein and Ginsburg, 2002); *L. observatum* (Korth and Evander, 2016); *L. anthrace* Cailleux et al., 2020.

Occurrence.—Early to late Miocene of Europe (Villalta and Crusafont, 1944; Baudelot and Crouzel, 1976; Mein and Ginsburg, 2002; Ziegler, 2005b, 2006b); middle to late Miocene of Asia and North America (James, 1963; Engesser, 1972; Storch and Qiu, 1991; Korth and Evander, 2016; Cailleux et al., 2020).

Lantanotherium sanmigueli Villalta and Crusafont, 1944
Figures 5–7; Table 2

Holotype.—Fragment of left mandible with m1 and m2, unnumbered, ICP, Viladecavalls, Spain (Villalta and Crusafont, 1944).

Diagnosis.—Small-sized *Lantanotherium* (m1 length of the holotype: 2.4 mm) characterized by the following combination of features: large I1; lack of diastema separating the upper and lower premolars; subtriangular P3 usually with a slight lingual extension; M1 and M2 with crescent metaconule; on M3, metacone and hypocone fused or distinct; usual presence of a reduced p1; narrow p4.

Occurrence.—MN9, MN10, and MN11 of Europe (Villalta and Crusafont, 1944; Ziegler, 2006a; Ménouret and Mein, 2008; Jablonski et al., 2014; Vasileiadou and Doukas, 2021); MN12 of Asia (Storch and Qiu, 1991).

Description.—The P3 is a small, triple-rooted tooth. The conical paracone is situated in a slightly anterior position; it is connected to a low metacone by a concave crest in occlusal view. A clear lingual extension bearing a small protocone is present (Fig. 5.1). From this cusp descends a low crest closing the anterolingual margin of the tooth. The labial part of P4 shows a relatively low, conical paracone, connected to the distinct parastyle by a faint ridge. The lingual extension has a rectangular outline with straight margins. A low crest along the anterior margin is connected to the protocone. The low hypocone is connected to a distinct posterior crest following the slight curvature of the posterolingual corner. A short, barely visible crest is found at the labial flank of the hypocone. Similarly, a hardly distinguishable V-shaped crest connects the lingual base of the hypocone to the lingual base

https://doi.org/10.1017/jpa.2023.50 Published online by Cambridge University Press

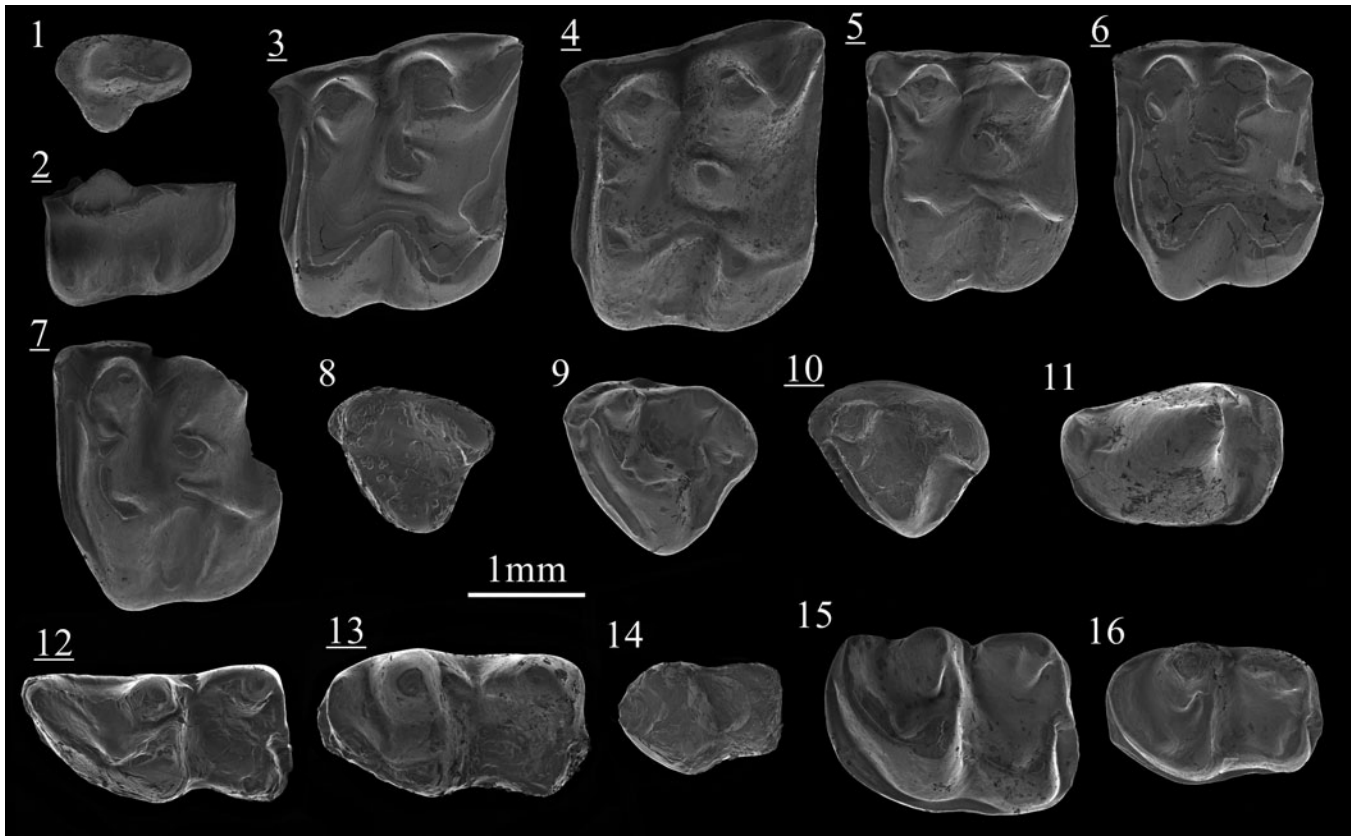

Figure 5. Scanning electron photomicrographs of *Lantanotherium sanmigueli* Villalta and Crusafont, 1944 from Borský Svätý Jur (**8, 12–14**), Studienka A (**1–7, 15, 16**) and Krásno (**9–11**): (**1**) P3, ST214001; (**2**) P4 (fragment), ST214220; (**3**) M1, ST214003; (**4**) M1, ST214221; (**5**) M2, ST214000; (**6**) M2, ST214004; (**7**) M2, ST214222; (**8**) M3, BJ213000; (**9**) M3, KR127012; (**10**) M3, KR127013; (**11**) p4, KR127014; (**12**) m1, BJ213001; (**13**) m2, BJ213002; (**14**) m3, BJ213003; (**15**) m2, ST214006; (**16**) m3, ST214224. Images with underlined numbers are reversed.

of the protocone. The dP4 is more gracile than the P4 (Fig. 6). The paracone is high and conical; a thin posterocrista connects it to the narrow posterior cingulum. The parastyle is small and independent from the paracone. The lingual area has two distinct cusps in anterior position. The protocone is smaller and in a less lingual position than the hypocone. The paracone is connected to the parastyle and the hypocone to the posterior cingulum.

The M1 is a sturdy, square-shaped molar with four roots. The metacone is wider than the paracone. A low metastyle is included in a short but broad postmetacrista connected to the metacone. The conical paracone is connected to the latter by a short, low, and straight ectoloph. From the anterior side of the paracone, a crest descends leading to a parastyle at the corner of the tooth. The protoconule is distinguishable within the protocone crest; it is not connected to the paracone, but to the paracone-parastyle crest at the base of the paracone. The protocone is as strong as the metacone and presents a robust triangular base; it is connected to a low and conical hypocone by a curved loph. From the posterior side of the hypocone descends a crest closing the posterior margin of the molar. The slightly crescent metaconule is isolated from the protocone and weakly connected to the metacone (Fig. 5.3, 5.4); it is higher than the hypocone. The inner basin thus corresponds to a valley compressed between the metaconule and the paracone. On the opposite side, the posterior basin is enlarged. The anterior cingulum is wide and starts from the base of the protocone. The labial cingulum is discontinuous. There is no cingulum on the lingual side.

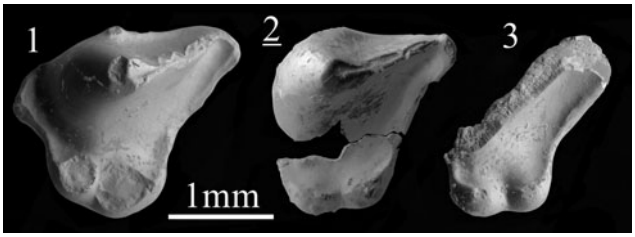

Figure 6. Scanning electron photomicrographs of the dP4 of *Lantanotherium sanmigueli* Villalta and Crusafont, 1944: (**1**) BJ213220; (**2**) ST214021; (**3**) ST214022. Image with underlined number is reversed.

The M2 is a compact and square tooth. The two lingual roots are fused at their bases. The postmetacrista is short and curvy. One of the specimens from Studienka A shows a posterolabial compression leading to an even shorter crest and a more rounded anterolabial corner (Fig. 5.6). The paracone is a conical cusp connected to the wider metacone by a low but sharp ectoloph; it is also connected to a small parastyle that veers labially to create a right anterolabial angle. The protocone is smaller than the metacone and the paracone and is connected to the hypocone by a curved crest. The protocone is connected to the paracone by a robust crest bearing a distinct protoconule. The posterior

https://doi.org/10.1017/jpa.2023.50 Published online by Cambridge University Press

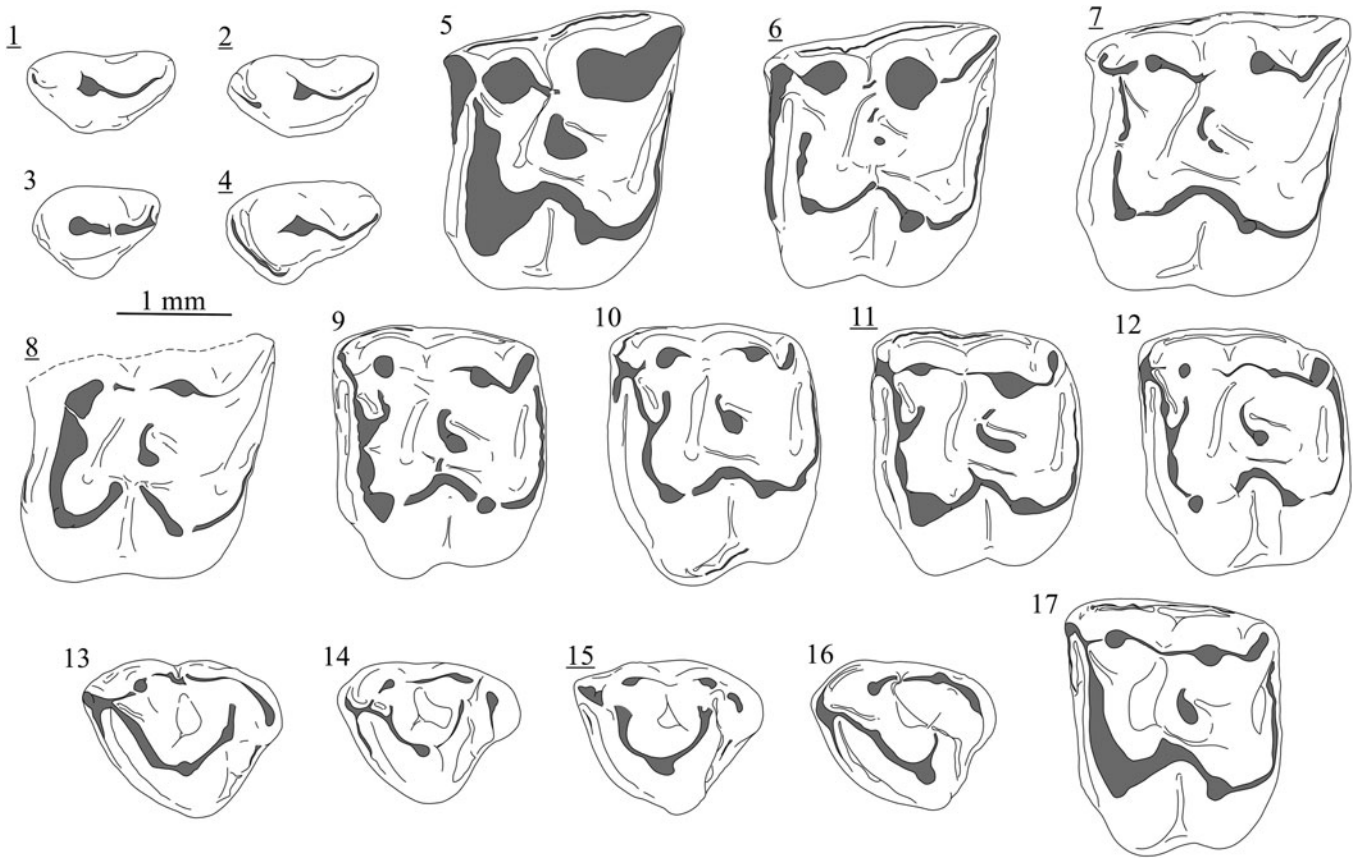

Figure 7. Variability of the dental elements of *Lantanotherium sanmigueli* Villalta and Crusafont, 1944 from Richardhof-Wald (**1–4**), Schernham (**5–16**), and Kohfidisch (**17**): (**1**) P3, Rh94/1-18A; (**2**) P3, Rh94/1-19A; (**3**) P3, Rh94/1-18B; (**4**) P3, Rh94/1-19C; (**5**) M1, SCH-3A; (**6**) M1, SCH-5C; (**7**) M1, SCH-2C; (**8**) M1, SCH-2B10; (**9**) M2, SCH-7D; (**10**) M2, SCH-4D; (**11**) M2, SCH-1F; (**12**) M2, SCH-8D; (**13**) M3, SCH-3H; (**14**) M3, SCH-1H; (**15**) M3, SCH-3I; (**16**) M3, SCH-2H; (**17**) M2, 2021/0049/0001. Images with underlined numbers are reversed.

postprotoconule notch is strong. The protocone-metaconule connection is absent, except in one specimen (Fig. 5.7) in which a low connection can be distinguished. The metaconule, slightly higher than the hypocone, is anteriorly connected to the base of the metacone. Anterior and posterior cingulums are large. The labial cingulum is narrower but complete and the lingual cingulum is very faint.

The M3 is a strong subtriangular tooth constituted by four cusps. The paracone is the strongest cusp, connected by a high, curved crest to the protocone and by a low crest to the metacone. Descending from the protocone, the posterior crest is weaker and does not reach the top of the hypocone; this crest is straight in three specimens (e.g., Fig. 5.10) and curved in one (Fig. 5.9). In a similar way, the metacone and hypocone are fused as a crescent crest in three specimens and are slightly separated in one. Anterior and posterior cingulums are present.

The p1 is a one-rooted, subtriangular unicuspid with no cingulid. The main cusp is situated in the middle of the premolar and continues as a low, curved bulge to the anterolingual border of the tooth; a thin crest connects the cusp to a low bulge situated

Table 2. Measurements (in mm) of *Lantanotherium sanmigueli* Villalta and Crusafont, 1944 from the late Miocene of Slovakia. L = length; L1 = labial length; L2 = shortest anteroposterior length; W = width; W1 = anterior width; W2 = posterior width.

	P3		DP4			M1			M2			M3			c	
	L	W1	L	W1	W2	L	W1	W2	L	W1	W2	L1	L2	W	L	W
N	1	1	1	1	1	3	3	3	2	3	2	4	4	4	1	1
Min	-	-	-	-	-	2.24	2.29	2.41	1.77	2.19	2.10	1.60	1.36	1.38	-	-
Max	-	-	-	-	-	2.32	2.38	2.67	1.80	2.33	2.13	1.90	1.46	1.61	-	-
Mean	1.18	0.88	1.75	0.85	1.03	2.28	2.33	2.50	1.78	2.26	2.11	1.72	1.42	1.49	1.23	0.82

	p1		p4		m1			m2			m3		
	L	W	L	W	L	W1	W2	L	W1	W2	L	W1	W2
N	1	1	1	1	1	2	2	2	3	6	3	6	5
Min	-	-	-	-	-	1.19	1.31	2.28	1.30	1.28	1.67	0.97	0.81
Max	-	-	-	-	-	1.37	1.32	2.31	1.45	1.50	1.88	1.27	1.16
Mean	0.79	0.59	1.98	1.26	2.42	1.28	1.31	2.29	1.36	1.43	1.78	1.14	1.04

https://doi.org/10.1017/jpa.2023.50 Published online by Cambridge University Press

at the posterolabial border. The p4 has a low conical and isolated paraconid in an anterolingual position. The protoconid is a sturdy cusp situated in the middle of the tooth. A small crest descends lingually without reaching the talonid; it ends as a small bulge (metaconid) at the base of the cusp. A low posterior crest—higher in its central part—surrounds the talonid; a feeble transverse crest starts from the central part and fades out at the base of the protoconid.

The m1 is a narrow tooth with an elongated trigonid. The lowest cusp of the trigonid is the paraconid, included in a long, bipartitioned paralophid connected to the protoconid; the latter is a high triangular cusp, weakly connected to a medium-sized, rounded metaconid by a notched protolophid. The trigonid basin is very narrow, but still largely open on the labial side of the tooth. The square-shaped talonid consists of a deep, almost-closed basin. The entoconid is pointed and only slightly smaller than the metaconid. The entocristid is a short, high crest that slopes down abruptly. A short metacristid is present (Fig. 5.12). On the posterior side of the entoconid runs a crest that splits into two arms in the middle of the posterior margin of the tooth; the first one reaches the hypoconulid whereas the second connects to a postcingulid reaching the posterolabial corner of the tooth. The hypoconid is the lowest cusp of the tooth; from it descends a straight oblique cristid decreasing in size anteriorly. The anterolabial cingulid is well developed. A short, narrow anterolingual cingulid is distinguishable between the paraconid and the metaconid. The m2 differs from the m1 mainly by the compressed trigonid, leading to a shorter paralophid and deeper trigonid basin. The metaconid is higher than the protoconid. The talonid is longer in m2 than in m1 (compare Fig. 5.12, 5.13). The anterior crest of the low hypoconid is less transversely directed. The postcingulid is connected to a low postcristid in all the four specimens. The labial cingulid is continuous. The m3 has a trigonid longer and slightly wider than the talonid, with a conical metaconid and a more anteroposteriorly compressed protoconid. The paraconid-metaconid connection is variable. The crest descending from the paraconid touches the base of the metaconid but usually does not complete the closure of the trigonid basin. Rarely, a short oblique crest starts from the metaconid and ends in the middle of the trigonid. The valley appears as a hook. A strong entoconid and a short but high entocristid characterize the square-shaped talonid. The oblique cristid is almost parallel to the entocristid. A reduced posterior cingulid is present in one of the two specimens in which this character could be observed.

Materials.—Borský Svätý Jur: one dP4, M3, one m1, one m2, two m3. Studienka A: one P3, one P4, two dP4, three M1, three M2, one M3, one c, two m1, four m2, three m3. Triblavina: one P4, one p1, one m3. Krásno: one M2, two M3, two p4, two fragments of m2, one m3. See Table 2 for measurements.

Remarks.—The species name *Lantanotherium sanmigueli* has been used to designate all of the small *Lantanotherium* from the late Miocene. This is partly a consequence of limited type material and a vague original description, making the data available poorly suited for comparisons. Moreover, the type material is a fragment of a mandible with m1 and m2 (Villalta and Crusafont, 1944) that does not show any diagnostic features except a size smaller than other European species. Ziegler (2006b), for instance, considered *L. sanmigueli* a nomen dubium. It is still unclear whether all of the material assigned to *L. sanmigueli* represents a single species. As a result, this has led to seeing this species as conservative, whereas relatively large variation is distinguishable in the plentiful European material (Furió et al., 2011b). Pending a study on the homogeneity of *L. sanmigueli,* we provide here an emended diagnosis sensu lato. The main distinctions among *Lantanotherium* spp. have been summarized by Cailleux et al. (2020; Table 1).

Lantanotherium sanmigueli is a very common taxon of the European late Miocene (Furió and Alba, 2011). Direct comparisons with material from Austria (Götzendorf, Richardhof-Golfplatz, Richardhof-Wald, Schernham, Eichkogel), France (Lo Fournas 1993, Montredon), and Spain (Can Llobateres 1) reveal relative homogeneity in size, but exceptions are found. This is the case for the relatively large specimens from the MN10 locality of Soblay and the more gracile elements from Borský Svätý Jur.

Lantanotherium sanmigueli is known for its wide morphological variability (Furió et al., 2011a). The presence of a minute protocone on a P3 from Studienka A is a feature only mentioned in non-Eurasian members of the genus (see Cailleux et al., 2020). P3 usually shows a slight or no lingual extension (Fig. 7.1–7.4). However, it is worth noting that no lacteal P3 of *Lantanotherium* is known, or at least has been identified as such. It is conceivable that the most reduced P3 of *L. sanmigueli* (e.g., Fig. 7.1, 7.2) represent decidual elements. This would be consistent with the overall smaller size and more reduced lingual region of the dP3 compared to the P3 in modern Erinaceinae and Hylomyinae (e.g., Butler, 1948; Engesser and Jiang, 2011; Voyta, 2017).

Three isolated elements from Borský Svätý Jur and Studienka A are attributed to the dP4 (Fig. 6), an element never described before in *Lantanotherium*. These teeth, for a long time unidentified in our material, share strong affinities with erinaceids. They are more gracile than in Erinaceinae and display a more reduced lingual configuration than in known dP4 of Galericini (e.g., Engesser, 1980; Ziegler, 1983). On the other hand, they still preserve lingual cusps, unlike the dP3 of known Galericini. These premolars are smaller than the P3, P4, and dP4 of *Schizogalerix voesendorfensis* and do not show any oblique orientation or angular aspect. Moreover, *L. sanmigueli* is the only Erinaceidae identified in both Borský Svätý Jur and Studienka A. Noticeable similarities are found between this element and the dP4 of the Recent Hylomyini *Neotetracus sinensis* Trouessart, 1909, of which the dental similarities with *Lantanotherium* were already noted (see Viret, 1940; Engesser and Jiang, 2011).

The protocone-hypocone loph on M1 is almost always complete and slightly curved, but the assemblage of Schernham yielded M1 with clearly curved loph. Within the 24 complete M1 from Schernham, two have a divided lophs (e.g., Fig. 7.8), which is a remarkable character only recorded in *Lantanotherium robustum* from La Grive (Mein and Ginsburg, 2002, fig. 25). One of the specimens of Studienka A shows a low protocone-metaconule connection (Fig. 5.7). This character

https://doi.org/10.1017/jpa.2023.50 Published online by Cambridge University Press

has never been previously described in *Lantanotherium*. We also observed that same crest in three of 24 M1 from Schernham (Fig. 7.6) and a central incomplete crest was also observed in the specimen from Rudabánya figured by Ziegler (2005b, pl. 1, fig. 8, MAFI V20504). Despite the fact that the rare occurrence of this probably ancestral morphotype is thus part of the broad qualitative variability of *Lantanotherium*, the common lack of the protocone-metaconule connection is still an important character to differentiate *Lantanotherium* from extinct to extant species of gymnures, e.g., *Neohylomys hainanensis* Shaw and Wong, 1959, *Neotetracus butleri* Mein and Ginsburg, 1997, and *Otohylomys megalotis* (Jenkins and Robinson, 2002).

One M2 from Studienka A (Fig. 5.6) stands out by its more compressed outline. Such a morphology has already been recorded in *Lantanotherium sanmigueli* specimens from the type locality of Viladecavalls (Furió et al., 2011b) and is also found in Richardhof-Wald and Schernham.

The fusion of the hypocone and metacone on the M3 of *Lantanotherium sanmigueli* (Fig. 7.13) is a feature frequently found during the Vallesian (e.g., Richardhof-Golfplatz, Studienka A), whereas these cusps are more clearly distinct in younger localities (e.g., Montredon, Krásno). The Schernham assemblage takes an intermediate position, with half of the M3 having a distinct hypocone and metacone (e.g., Fig. 7.14, 7.15). We observed that the lower molars from Borský Svätý Jur are narrow compared to the younger material from Studienka, Schernham, and Soblay. Such a shape is also found in the material of Lufeng (MN12; Storch and Qiu, 1991) and Eichkogel (MN11; Rabeder, 1973), which could indicate intraspecific variability. The latter locality yielded a p4 attributed to *L.* cf. *L. sanmigueli* by Rabeder (1973, fig. 28), which, however, seems to belong to a vespertilionid bat.

Subfamily Erinaceinae Fischer, 1814
Genus *Atelerix* Pomel, 1848

Type species.—*Erinaceus albiventris* Wagner, 1841.

Other species.—*Atelerix frontalis* (Smith, 1831); *Atelerix algirus* (Lereboullet in Duvernoy and Lereboullet, 1842); *Atelerix sclateri* Anderson, 1895; *Atelerix depereti* Mein and Ginsburg, 2002; *Atelerix rhodanicus* Mein and Ginsburg, 2002; and *Atelerix steensmai* Van Dam, Mein, and Alcalá, 2020.

Diagnosis.—See Frost et al. (1991, p. 31).

Occurrence.—Late-middle Miocene to late Miocene of Europe (Mein and Ginsburg, 2002; Ziegler, 2006b, 2006a); identified from the Plio-Pleistocene in Africa (Zouhri et al., 2017; Cailleux, 2021). Crespo et al. (2020) recorded cf. *Atelerix* from the early Miocene (MN3) of Mas d'Antolino B3, but this identification is based on a single M3, which is insufficient to allow identification beyond the subfamily level. The inclusion of *Mioechinus* Butler, 1948 into *Atelerix* would extend its geographical and temporal range (e.g., Qiu, 1996; Mein and Ginsburg, 1997; Li et al., 2019).

Remarks.—We consider here Miocene forms as *Atelerix*, but we are aware that such generic attribution is still uncertain. If extant Erinaceinae diversified during the late Miocene (Bannikova et al., 2014), it is not surprising to see slight differences between *Atelerix*, *Erinaceus* Linnaeus, 1758, and *Mioechinus*. Because there are only a few derived dental features allowing differentiation of modern *Erinaceus* from modern *Atelerix*, pinpointing the emergence of *Erinaceus* is also hardly possible. The taxonomy of this subfamily is largely based on cranial elements, which are exceedingly rare in the fossil record. We follow Ziegler (2005a) rather than Mein and Ginsburg (2002) in considering *Mioechinus* and *Atelerix* as separate taxa.

Atelerix cf. *A. depereti* Mein and Ginsburg, 2002
Figure 8.1, 8.2

Diagnosis.—See Mein and Ginsburg (2002, p. 14).

Occurrence.—The type locality of *Atelerix depereti* is the MN7/8 fissure filling L5 from La Grive Saint-Alban (Mein and Ginsburg, 2002).

Description.—Only the posterior part of the lower canine is preserved. The tooth is large and elliptical. From the main cusp descends a sharp crest reaching a small cuspule on the posterior border; from this cuspule runs a well-developed posterolingual cingulum. The posterolabial cingulum only corresponds to a small slope. The lower p3 is also only partially preserved (Fig. 8.1). This one-rooted tooth has an angular shape with one large but low main cusp. A bulge is present on the posterior border of the tooth, not connected to the main cusp. The posterior border is oblique. The fragment of p4 (Fig. 8.2) is characterized by a very narrow anterior part. The heavily worn paraconid is large; it is connected to the protoconid by a worn labial crest well differentiated from the narrow valley. There is no ectocingulid. The anterior face of the metaconid is robust.

The lower m2 has a well-developed trigonid basin. The paralophid and paraconid are fused into a single ridge, which bends at the lingual side and partly closes the trigonid basin. The latter cusp is strong and conical. A short, straight crest runs from its posterior part, reaching at least the middle part of the trigonid.

Materials.—Borský Svätý Jur: one fragment of c (W = 1.89), one fragment of p3, one fragment of p4, one fragment of m2 (W1 = 2.22).

Remarks.—Alone, the dental morphology of Erinaceinae has only feeble resolving power (Gould, 2001). Van Dam et al. (2020) made a comprehensive summary of what we know—and what we do not know—about the paleodiversity of Erinaceinae during the Miocene. Five genera are defined in Europe: *Amphechinus* Aymard, 1850, *Postpalerinaceus* Crusafont and Villalta, 1947, *Erinaceus*, *Atelerix*, and *Mioechinus*, the last being included in *Atelerix* by Mein and Ginsburg (2002). *Amphechinus* is an ancestral group that was not present in the late Miocene of central Europe (Gibert, 1975; Van Dam et al., 2020; Cailleux, 2021). This epoch was characterized by the success of *Postpalerinaceus vireti* in western Europe.

https://doi.org/10.1017/jpa.2023.50 Published online by Cambridge University Press

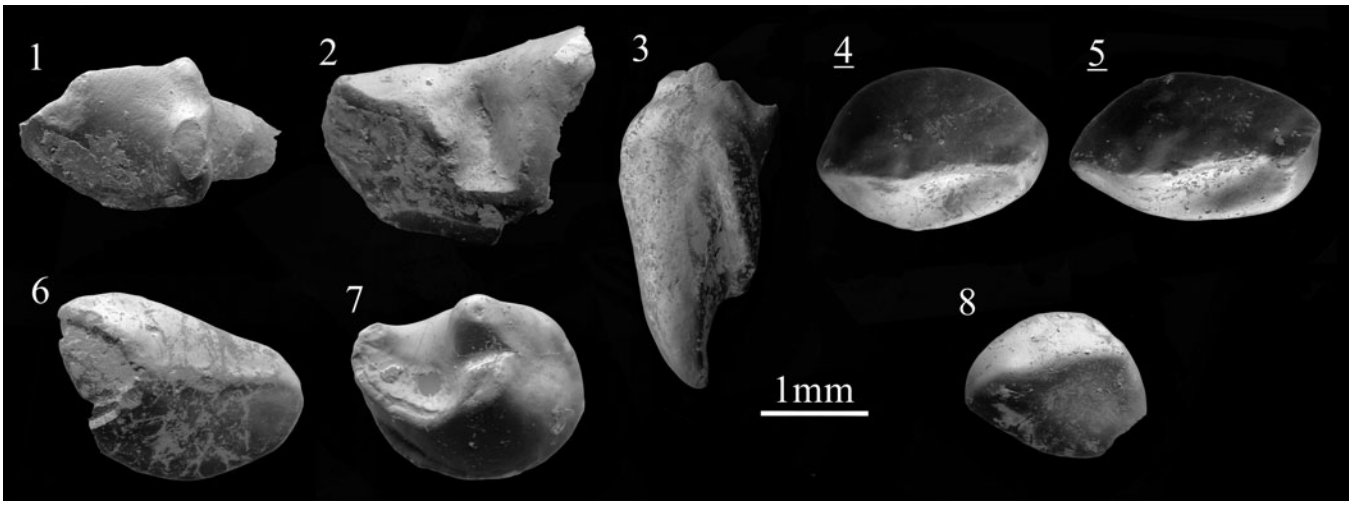

Figure 8. Scanning electron photomicrographs of *Atelerix* cf. *A. depereti* Mein and Ginsburg, 2002 (**1, 2**), *Atelerix* aff. *A. depereti* (**3–7**), and cf. *Postpalerinaceus* sp. indet. (**8**): (**1**) p3, BJ213006; (**2**) p4, BJ213006; (**3**) I2, KR127002, labial view; (**4**) P2, KR127000; (**5**) P2, KR127001; (**6**) i3, KR127007; (**7**) m3, SG198001; (**8**) I2, KR127006. Images with underlined numbers are reversed.

The form from Borský Svätý Jur is only known by fragments, whose dimensions correspond with a medium-sized species, e.g., *Atelerix depereti*. Our fragment of p4 is narrower than in *Postpalerinaceus cingulatus* Zeigler 2005b and does not present any noticeable trace of an ectocingulid. It also differs by its deep trigonid basin from most species, with the noticeable exception of *Atelerix rhodanicus, Atelerix depereti*, and the indeterminate Erinaceinae from Petersbuch 31 (Ziegler, 2005a, NHMA P31-137A3). The labial border of the p3 is transverse, which is a feature found in *Atelerix depereti* and in *Atelerix* aff. *A. depereti* from Spain (Mein and Ginsburg, 2002; Van Dam et al., 2020). Direct comparison with '?cf. *Atelerix depereti*' from Götzendorf (Ziegler, 2006b) revealed strong similarities with our material. Because Götzendorf and Borský Svätý Jur are close in age and from the same basin, the two samples probably correspond to a single species. Additionally, Erinaceinae gen. indet. sp. indet. 1 from the MN9 Moldovan locality of Buzor-1 (Rzebik-Kowalska and Lungu, 2009) shows strong similarities with our material and could correspond to a closely related form.

Atelerix aff. *A. depereti* Mein and Ginsburg, 2002
Figure 8.3–8.7

Description.—The I2 is a high, curved, one-rooted tooth; its crown and root are anteroposteriorly compressed. In the middle of the tooth, the only cusp has an elongated top with an anteroposterior orientation. The distal side is only composed of the strong slope of the main cusp whereas the mesial side is more complex. From the most posterior part of the cusp starts a curved crest strengthening the distal margin before ending on the anteromesial border of the tooth (Fig. 8.3). The oval I3 has a sturdy main cusp in an anterior position and an anteriorly elevated crown; from the cusp descends a ridge ending at the posterior border of the tooth. There is no distinct cingulid but the slope of the main cusp becomes smaller on the distal side of the specimen, leading to a more extended zone. The two roots show an oblique, backward orientation. The anterior root is smaller than the posterior one.

The posterior part of the upper canine presents a rounded outline. The main cusp is slightly inflated. A robust, central posterior crest is present, reaching the low, irregular posterior cingulum. The P2 has an ovoid to slightly elongated outline (Fig. 8.4, 8.5); the roots have not been preserved. The cusp is situated in an anterior position; it is included in a median crest crossing all of the premolar. At the most anterior margin, this crest turns lingually; at the back, it ends at the straight posterior margin of the tooth as a small bulge. The slight labial crest creates a concave posterolingual slope.

The i3 is an oval tooth similar in size to the P2 but with a more flattened crown. The main cusp is situated at the anterior margin. A crest crosses the incisor obliquely to reach the posterodistal border.

The broken m2 is only known by a lingual fragment. We mainly note a conical metaconid, from which a notched protolophid descends labially. A notch is found in the middle of the protolophid. The cuspid is enlarged. The complete m3 is elliptical. It mostly consists of the long paralophid in which the paraconid is not distinct. The metaconid is slightly stronger than the protoconid. They are set close together, implying a short protolophid. The trigonid basin is deep and widely open (Fig. 8.7). A narrow anterolabial cingulid is distinguishable.

Materials.—Krásno: one I2 (L = 1.53, W = 1.46), one fragment of C, two P2 (L = 2.20, W = 1.53; L = 2.28, W = 1.38), one i3 (L = 2.06, W = 1.51). Šalgovce 5: one I3 (L ≃ 2.56, W = 1.66), one fragment of m2 and one m3 (L = 2.17, W = 1.73).

Remarks.—All specimens described here correspond to a medium-sized erinaceine considered to represent a single species. The I2 from Krásno (KR127006) presents a shape found in *Atelerix* and is similar to the I2 of *Atelerix* aff. *A. depereti* described by Van Dam et al. (2020; ROM 7-259, from Masia de la Roma, Teruel Basin, central Spain), despite being larger and having a stronger cingulum. The I2 of

https://doi.org/10.1017/jpa.2023.50 Published online by Cambridge University Press

Erinaceus samsonowiczi Sulimski, 1959 from Maramena is even larger and more massive (unpublished data, F. Cailleux, 2021). The I3 from Šalgovce 5 is easily distinguishable from the caniniform I3 of *Amphechinus* (see Viret, 1938) and presents a more advanced flattening stage than *Postpalerinaceus intermedius* from La Grive (Mein and Ginsburg, 2002) and '*Mioechinus*' *tobieni* Engesser, 1980 from Eskihisar (Engesser, 1980). Our specimen is similar in shape to the material of *Atelerix depereti* described by Mein and Ginsburg (2002) but is slightly larger. *Atelerix* aff. *A. depereti* described from MN9-12 localities of Spain (Van Dam et al., 2020) have an I3 which corresponds in size and displays an oblique orientation. The median crest of our specimen is, however, less marked. The size of the P2 from Krásno falls into the lowermost variability of *Atelerix* aff. *A. depereti* but in the center of the variability of *Atelerix depereti*, the latter having less massive teeth, like our specimens. The dimensions of the m3 are found in the upper variability of *Atelerix depereti* from La Grive (Mein and Ginsburg, 2002) and the lower variability of *Atelerix* aff. *A. depereti* from the Turolian of Spain (Van Dam et al., 2020).

The material from Krásno and Šalgovce 5 fits well with *Atelerix* aff. *A. depereti* as described from MN9-12 localities in Spain (Van Dam et al., 2020). This form overall shows a larger size and proportionally wider elements than the type material of *Atelerix depereti*. According to Van Dam et al. (2020), the development of the lingual extension on P2, leading to a width increase, occurred during the *Atelerix depereti-Atelerix* aff. *A. depereti* lineage.

Genus *Postpalerinaceus* Crusafont and Villalta, 1947

Type species.—*Postpalerinaceus vireti* Crusafont and Villalta, 1947.

Other species.—*Postpalerinaceus intermedius* (Gaillard, 1899); *Postpalerinaceus cingulatus* Ziegler, 2005b.

Occurrence.—*Postpalerinaceus* is recorded from the late-middle Miocene and the late Miocene of Europe (Mein et al., 1990; Mein and Ginsburg, 2002; Ziegler, 2005b, Van Dam et al., 2020).

cf. *Postpalerinaceus* sp. indet.
Figure 8.8

Description.—The I2 from Krásno is a rounded monocuspid tooth with only a slightly asymmetrical shape. The main cusp is included in a median crest. The distal side is inflated whereas the mesial one is anteriorly straight and posteriorly concave. The median crest ends posteriorly by joining a small posterodistal cingulum.

Materials.—Krásno: one I2 (L = 1.41, W = 1.49).

Remarks.—The structure of the I2 can be distinguished from the morphology of *Amphechinus*, *Atelerix*, and *Mioechinus*, in which the crown is more elevated and complex. Our specimen fits the configuration of *Postpalerinaceus* (see Crusafont and Villalta, 1947). The specimen from Krásno is smaller than the I2 of the holotype of *Postpalerinaceus vireti* but falls within the size variability of *Postpalerinaceus* cf. *P. vireti* from the Teruel Basin (Van Dam et al., 2020) and in the lower part of the *Postpalerinaceus intermedius* variability from La Grive (Mein and Ginsburg, 2002). Morphologically, the Krásno tooth resembles either species. *Postpalerinaceus* is poorly recorded in central Europe. The only identified species, *Postpalerinaceus cingulatus* from the MN9 locality of Rudabánya (Ziegler, 2005b), is distinctively smaller than western European species. We note the possible occurrence of *Postpalerinaceus* in the Austrian MN10 locality of Schernham, Austria (Ziegler, 2006b), which suggests the presence of a medium-sized species, at least similar to *Postpalerinaceus,* during the late Vallesian and early Turolian of central Europe.

Erinaceinae gen. indet. sp. indet.

Description.—A large fragment of an upper canine from Šalgovce 5 shows a main cusp with an inflated tip. A marked posterior crest starts from the top of the cusp and joins the posterior shoulder. A fainted posterior cingulum is present, broader on the lingual side.

Materials.—Šalgovce 5: one fragment of C (W ≈ 2.49).

Remarks.—The morphology of the canine fits with the usual morphology of upper canine in erinaceines. Its size, however, does not correspond with the known dimensions of *Atelerix depereti* or *Atelerix* aff. *A. depereti*, but rather fits with larger species, e.g., *Postpalerinaceus vireti* and *Atelerix steensmai*.

Family Dimylidae Schlosser, 1887
Genus *Plesiodimylus* Gaillard, 1897

Type species.—*Plesiodimylus chantrei* Gaillard, 1897.

Other species.—*Plesiodimylus huerzeleri* Müller, 1967; *Plesiodimylus crassidens* Engesser, 1980; *Plesiodimylus bavaricus* Schötz, 1985; *Plesiodimylus helveticus* Bolliger, 1992; *Plesiodimylus johanni* Kälin and Engesser, 2001; *Plesiodimylus gaillardi* Mein and Ginsburg, 2002; *Plesiodimylus similis* Fejfar and Sabol, 2009; and *Plesiodimylus ilercavonicus* Crespo et al., 2018.

Diagnosis.—See Fejfar and Sabol (2009, p. 612), translation from Müller (1967).

Occurrence.—Early to late Miocene of Europe and Anatolia (Engesser, 1980; Doukas, 1986; Fejfar and Sabol, 2005, 2009; Ziegler, 2006a; Klietmann et al., 2014b; Van den Hoek Ostende and Fejfar, 2015; Crespo et al., 2018).

Plesiodimylus chantrei Gaillard, 1897
Figure 9.1–9.15; Table 3

Holotype.—Fragment of left mandible with p2–m2, La Grive 208b, La Grive Saint-Alban, France (Gaillard, 1899).

https://doi.org/10.1017/jpa.2023.50 Published online by Cambridge University Press

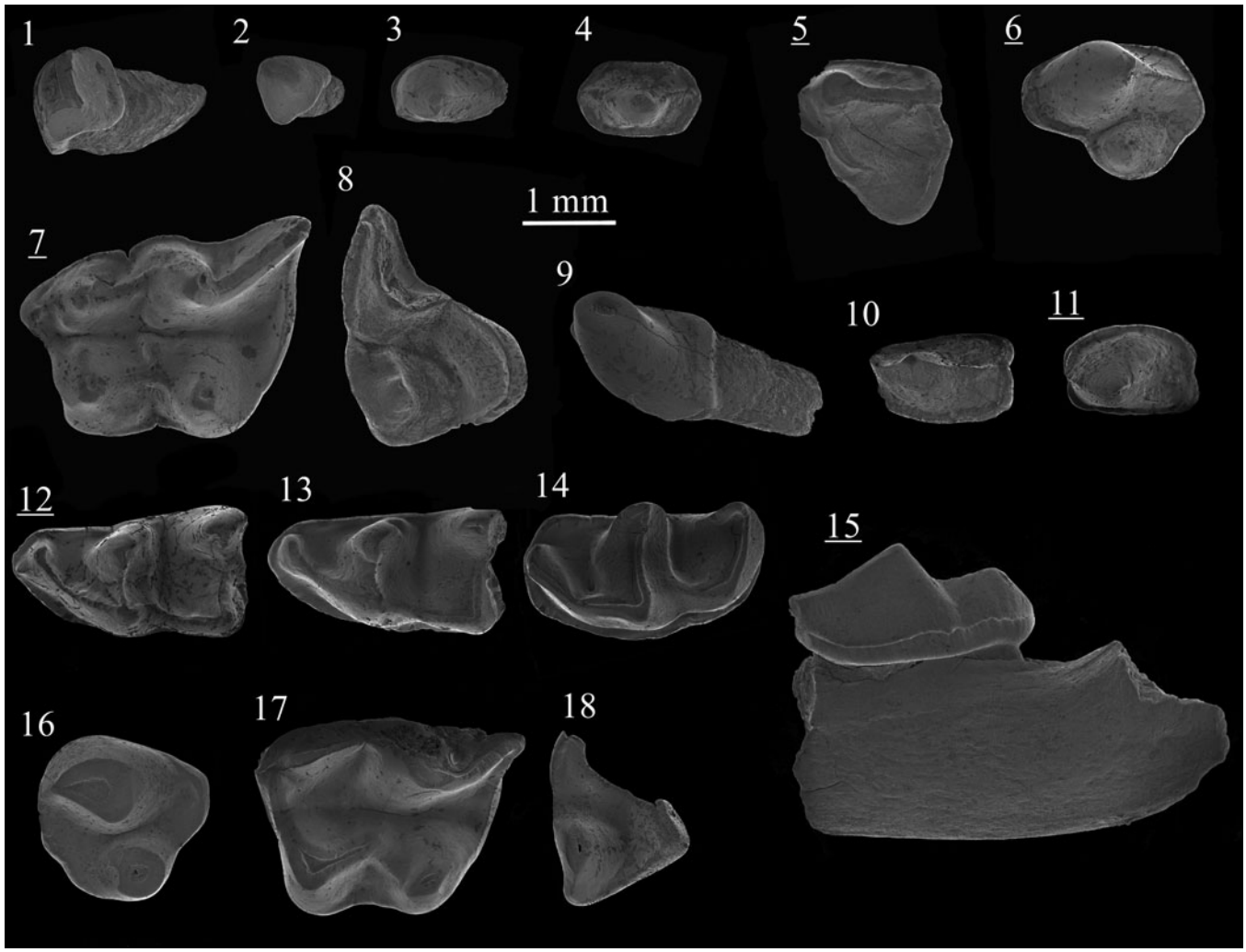

Figure 9. Scanning electron photomicrographs of *Plesiodimylus chantrei* Gaillard, 1897 (**1–15**) and *Metacordylodon* aff. *M. schlosseri* (Andreae, 1904) (**16–18**) from Studienka A (**1–4**, **6–18**) and Studienka E (**5**): (**1**) I1, ST214093; (**2**) I2/3, ST214094; (**3**) C, ST214102; (**4**) P1, ST214095; (**5**) DP4, ST214211; (**6**) P4, ST214107; (**7**) M1, ST214060; (**8**) M2, ST214087; (**9**) i1, ST214122; (**10**) p1, ST214125; (**11**) p4, ST214129; (**12**) m1, ST214115; (**13**) m1, ST214119; (**14**) m2, ST214134; (**15**) mandible with m2, ST214140; (**16**) P4, ST214052; (**17**) M1, ST214050; (**18**) M2, ST214051. Images with underlined numbers are reversed.

Diagnosis.—See Fejfar and Sabol (2009, p. 612).

Occurrence.—Early to late Miocene of Europe (Gaillard, 1897; Rzebik-Kowalska, 1996; Ziegler, 2005b, 2006b; Klietmann et al., 2014b). The type locality of *Plesiodimylus chantrei* is La Grive-Saint-Alban (MN7+8, France). Gaillard (1897) did not mention the fissure from which the holotype was extracted, but the work of Chantre and Depéret at the end of the nineteenth century was focused on the Peyre et Beau quarry (Mein and Ginsburg, 2002).

Description.—I1/I2 is a simple triangular tooth bearing no cingulum. It has a pointed cusp. The mesial and posterior faces are flat and the anterodistal is convex. The root is almost straight, semicircular in cross section with a flat mesial face. I3 is a small monocuspid tooth that is labiolingually compressed. The subtriangular crown bears a short median crest. Two short extensions are found on either side, the lingual one running at a lower level than the labial one. The rounded root is posteriorly orientated.

The upper canine is a two-rooted, almond-shaped tooth with a caniniform cusp. The posterior crest connects the cusp with the posterior border of the narrow but complete cingulum. The P1 has a subhexagonal outline (Fig. 9.3). The cusp is situated in the center of the tooth. Low anterior and posterior crests descend from it, reaching the complete cingulum at the anterior and posterior border, respectively; these crests have a slightly labial position. Two thin but well-separated roots are present with a posterior orientation. The P4 is a three-rooted tooth with an elongated labial margin. The large and oval paracone is in an anterolabial position. From it descends a robust but low crest that reaches a straight oblique wall at the posterior margin of the tooth. The protocone is conical, situated on the lingual side in a more central position than the paracone; its posterior slope is extended, leading to a small and narrow basin. The P4 is surrounded by an almost complete, thick cingulum, interrupted at the base of the protocone. The dP4 is distinguishable by its more irregular outline (Fig. 9.5). The paracone is weaker than in the P4 and connected to a blade-like protocone. Due to the wide posterolingual extension, the lingual basin is larger than in P4.

https://doi.org/10.1017/jpa.2023.50 Published online by Cambridge University Press

Table 3. Measurements (in mm) of *Plesiodimylus chantrei* Gaillard, 1897 from the late Miocene of Slovakia. L = length; W = width; W1 = anterior width; W2 = posterior width.

	I1/I2		I3		C		P1		DP4	P4		M1		M2		c	
	L	W	L	W	L	W	L	W	L	L	W	L	W	L	W	L	W
N	1	1	1	1	7	8	4	5	1	8	7	2	5	9	5	2	2
Min	-	-	-	-	1.21	0.72	1.20	0.78	-	1.91	1.46	3.28	2.28	1.71	2.45	1.29	1.13
Max	-	-	-	-	1.34	0.78	1.33	0.91	-	2.04	1.59	3.36	2.39	1.94	2.62	1.32	1.14
Mean	0.99	1.23	0.71	0.81	1.28	0.76	1.28	0.82	1.70	1.99	1.51	3.32	2.35	1.84	2.55	1.31	1.13
	p1		p2/p3		p4		m1			m2							
	L	W	L	W	L	W	L	W1	W2	L	W1	W2					
N	2	1	1	2	3	3	5	7	7	8	6	6					
Min	1.56	-	-	0.77	1.52	0.95	2.54	1.18	1.32	2.47	1.36	1.12					
Max	1.57	-	-	0.78	1.61	0.99	2.77	1.40	1.56	2.73	1.42	1.22					
Mean	1.56	1.00	0.63	0.78	1.57	0.98	2.63	1.29	1.41	2.62	1.39	1.17					

The M1 is a massive subrectangular tooth with five roots and three basins. The large metacone is connected to an indistinct metastyle by a wide postmetacrista. The postparacrista reaches the flank of the metacone. Together with the protocone, the parastyle, which is connected to the base of the paracone, forms a small anterior basin. The protocone is almost as large as the hypocone and connected to it by a low crest. The prehypocrista is shorter and weaker than the postprotocrista. The hypocone has a more lingual position than the protocone. On its posterior side, a deep basin is bordered by a robust cingulum reaching the base of the metastyle. Thin cingula are distinguishable all along the anterior margin of the tooth, and between the protocone and the hypocone. In occlusal view, a short central notch is usually observed on both labial and lingual cingulums. The three-rooted M2 displays a wide and isolated protocone, occupying a significant part of the occlusal surface. A valley separates the protocone from the other cusps. The metacone is not differentiable from the straight premetacrista and the curved postmetacrista. Mesostyles are only slightly divided on the most unworn specimen. The paracone is more distinct than the metacone because the postparacrista and the preparacrista are relatively reduced. The first crest is S-shaped when reaching the parastyle. A short cingulum is present lingual to the parastyle. A shorter one is distinguishable between the mesostyle and the parastyle.

The lower canine is a robust, almond-shaped, one-rooted tooth with a strong cuspid in an anterior position. A small bulge is found on the anterior face of this cuspid. The posterior part only bears a faint cingulum. The posterolabial slope is reaching lower than the posterolingual one. The p1 is an elliptical, two-rooted tooth with a relatively wide posterior part; it is the largest lower premolar. The main cuspid is placed in a more anterior position; from it descends an anterior crest that turns lingually, and a weaker posterior crest that reaches the middle of the posterior margin. A continuous cingulid is present. The one-rooted p2/p3 is wider than long, with two lobes. The cuspid is found in an anterior position and is included in a crest reaching the anterior border. An almost complete cingulid is present, except for on the most posterior part of the tooth, at which the outline is slightly concave. The p4 is slightly shorter than p1 (compare Fig. 9.11, 9.10) and has an angular shape. The main cuspid has a subtriangular base and from its top descends a short anterior crest but no posterior crest. A cingulid is present all around the premolar except below the anterior crest. In one out of three specimens, the cingulum is connected to this crest.

The m1 is a robust tooth with a narrow trigonid. The valley of the trigonid basin is weak and oblique. The low blade-like paraconid is transversly oriented and connected to the protoconid by a bipartitioned paracristid. In two of seven specimens, a low accessory cuspid is attached to the paracristid (Fig. 9.12). The protoconid is a stout, bulbous cuspid. The metaconid has the same height but is less wide. The cuspids are connected to each other by a short, straight protocristid. The talonid basin is longer and wider than the trigonid one; it is less lingually opened. The entoconid is high with no anterior crest, whereas the hypoconid is lower and wider. A robust oblique cristid runs from the hypoconid; this straight crest reaches the base of the protoconid. A postcingulid is connected to the postcristid

Table 4. Composition of the Erinaceidae and Dimylidae from the late Miocene of Slovakia (in N of identified specimens).

	MN9				MN10	MN11		MN12
	Borský Svätý Jur	Studienka			Pezinok	Triblavina	Krásno	Šalgovce 5
		A	BC	E				
Erinaceidae								
'*Schizogalerix' voesendorfensis* (Rabeder, 1973)	200	-	-	-	-	-	-	-
Schizogalerix cf. *S. moedlingensis* (Rabeder, 1973)	-	-	-	-	-	-	10	-
Lantanotherium sanmigueli Villalta and Crusafont, 1944	6	24	-	-	-	3	7	-
Atelerix cf. *A. depereti* Mein and Ginsburg, 2002	4	-	-	-	-	-	-	-
Atelerix aff. *A. depereti* Mein and Ginsburg, 2002	-	-	-	-	-	-	5	3
cf. *Postpalerinaceus* sp. indet.	-	-	-	-	-	-	1	-
Erinaceinae gen. indet. sp. indet.	-	-	-	-	-	-	-	1
Dimylidae								
Plesiodimylus chantrei Gaillard, 1897	-	84	10	9	3	1	-	-
Metacordylodon aff. *M. schlosseri* (Andreae, 1904)	-	3	-	-	-	-	-	-

https://doi.org/10.1017/jpa.2023.50 Published online by Cambridge University Press

or to the entoconid. The cingulid is continuous except between the metaconid and the entoconid. In two of three specimens, a second short cingulid is distinguishable. In the m2, deep valleys separate high ridges in which cuspids are sometimes not distinguishable. The paraconid corresponds to a compressed bulge in the high, transverse paracristid. The metaconid and the protoconid are similar in morphology and are smaller than the protoconid; they are connected to each other by a high protocristid. The trigonid basin is longer than in the m1 and the talonid basin is much more rounded. The two talonid cuspids are fused with the oblique cristid as a single long, convex crest. The cingulid runs from the base of the metaconid to the center of the talonid posterior margin. A bulge is situated on the anterolingual side of the cingulid, near the paraconid.

Materials.—Studienka A: one I1/2, one I3, eight C, five P1, 10 P4, 20 M1, 13 M2, two c, four p1, one p2/p3, two p4, nine m1, nine m2. See Table 3 for measurements. Studienka BC: two C (L = 1.28, W = 0.77; L = 1.29, W = 0.76), one P4 (L = 1.97), three M1, three M2 (L = 1.86, 1.89, 1.94), one p2/p3 (L = 0.62, W = 0.77). Studienka E: one dP4 (L = 1.70), one P4 (L = 2.00), one p4 (L = 1.61, W = 0.99), three m1 (L = 2.77, W1 = 1.18, 1.33), three m2. Pezinok A: two m1 (L = 2.58, W1 = 1.40; W2 = 1.56), one m2 (L = 2.73, W 1 = 1.42, W2 = 1.19). Triblavina: one M1 (W = 2.30).

Remarks.—The described P1 are large and exceed the upper canine in size. The variability of this element was not previously mentioned in the literature. No P3 are recognized in our material. Similarly, Ziegler (2006b) did not report any P3 nor P1 from the rich Austrian localities. P3 are similar to P1 in size and shape but can be distinguished by the more anterior position of the cuspid and the reduction of the central anterior crest. However, this observation is based on the early Miocene material described by Klietmann et al. (2014b), which could present dissimilarities with younger forms. The recognition of some antemolar elements appears hardly possible without complete material (e.g., Viret, 1931; Seeman, 1938; Engesser, 2009).

Plesiodimylus chantrei is one of the most common Miocene insectivores because of both its high abundance and longevity, ranging from MN4 to MN11 (Klietmann, 2013; Van den Hoek Ostende et al., 2023), which also seems related to a generalist paleoecology. Its remarkable stratigraphical distribution led several workers to investigate the size and morphological homogeneity of *Plesiodimylus chantrei*, which did not support the division of this taxon (e.g., Engesser, 1972; Klietmann et al., 2015). Nevertheless, the various populations present a wide range of morphological and size variability. Ziegler (2006b) identified the material from Eichkogel as *Plesiodimylus* cf. *P. chantrei*, and the material from Götzendorf, Richardhof-Golfplatz, Richardhof-Wald, and Schernham as *Plesiodimylus* aff. *P. chantrei*. The use of the latter open nomenclature is related to the larger dimensions of the specimens from Austria, that almost reach the dimensions of the material from Nebelbergweg attributed to *Plesiodimylus johanni* by Kälin and Engesser (2001). *Plesiodimylus johanni* displays several morphological peculiarities, none of which are present in the Austrian and Slovak material (see Ziegler, 2006b). Moreover, the morphometric variability of *Plesiodimylus chantrei* and that of *Plesiodimylus johanni* are not perfectly separated (Kälin and Engesser, 2001, fig. 18). In the case of the Slovak material, there are no clear outliers as in Richardhof-Wald and Richardhof-Golfplatz, despite the mean measurements being higher than the usual mean measurements of *Plesiodimylus chantrei*. As in the case of Rudabánya (Ziegler, 2005b), the use of open nomenclature for our sample is considered unjustified.

Rzebik-Kowalska (1996) highlighted that there is no clear pattern in the size evolution of *Plesiodimylus chantrei*. This is in line with the model of Klietmann (2013), in which *Plesiodimylus chantrei* corresponds to a uniform, widespread taxon in which separated populations have emerged, resulting in new local species. Nevertheless, the central European late Miocene record (e.g., Ziegler, 2005b, 2006b; Fejfar and Sabol, 2009; this work) does show a tendency to larger variety. In that sense, despite some similarities with the older *Plesiodimylus crassidens*, *Plesiodimylus johanni* can be seen as a local MN9 morphological variant of an already large-sized population of *Plesiodimylus chantrei*. This hypothesis is still coherent with the model of Klietmann (2013) and the size dimorphism observed in the *Plesiodimylus* material from the MN7/8 fissure fillings of Petersbuch by Ziegler (2005a).

Genus *Metacordylodon* Schlosser, 1911

Type species.—*Cordylodon schlosseri* Andreae, 1904, by monotypy.

Occurrence.—Late-early Miocene to early-late Miocene of Europe (Andreae, 1904; Wegner, 1913; Viret, 1931; Crusafont-Pairó and Golpe, 1972; Fahlbusch, 1989; Ziegler, 2000, 2005a, b; Fejfar and Sabol, 2005).

Metacordylodon aff. *M. schlosseri* (Andreae, 1904)
Figure 9.16–9.18

Description.—The P4 is a robust ovoid tooth with three roots. A short crest starts on the posterior side of the massive paracone and ends abruptly on the posterior wall. A low posterior crest constitutes the straight anterolabial margin of the teeth. The large, conical protocone is situated in a more anterolingual position than the paracone. A posterolabical extension is present between the paracone and the posterior margin and consists of a weak slope.

The M1 is a massive molar with two basins. The labial side is not preserved (Fig. 9.17). The protocone is a massive subtriangular cusp connected by an anterior arm to a parastyle that lies in an anterolabial position. The anterior basin is deep and circular. The protocone is connected to the hypocone by a reversed V-shaped crest. The prehypocrista is weaker than the postprotocrista. The hypocone is smaller than the protocone and has an oblique orientation. The posterior cingulum is narrow, bordering a posterior basin less deep and larger than the anterior one. A short lingual cingulum is present between the protocone and the hypocone. The incomplete M2 has a subtriangular outline. The protocone is wide, anteroposteriorly compressed, and separated from the other cusps by a wide valley. A short crest descends from the lingual side of the protocone, leading to a

https://doi.org/10.1017/jpa.2023.50 Published online by Cambridge University Press

small bulge on the anterolingual corner of the tooth. The postmetacristra is straight and connects the base of the protocone to a low metacone. The latter cusp creates a right angle at the posterolingual corner. The premetacrista is higher and larger than the postmetacrista. A short cingulum is partly preserved on the posterolabial margin.

Materials.—Studienka A: one P4 (L = 1.87, W = 1.80), one broken M1 (L > 2.94), one broken M2 (L = 1.46).

Remarks.—*Metacordylodon* is a very rare member of late Miocene fauna. Mainly recorded during the middle Miocene, this genus was also recorded in the early Miocene of Sandelzhausen and Franzensbad (Ziegler, 2000). The late Miocene records include Schernham, Richardhof-Golfplatz (Ziegler, 2006b), and Rudabánya (Ziegler, 2005b). At the latter locality, the material was attributed to a small form named *Metacordylodon* aff. *M. schlosseri*. Our material is significantly smaller than middle Miocene material but only slightly smaller than the P4 (MAFI V20525) and the M1 (MAFI V20524) specimens described from Rudabánya. Our P4 (Fig. 9.16) is significantly smaller than the one from Richardhof-Golfplatz (Ziegler, 2006b; RH-A2-C11) and does not present a distinct anterior cuspule. There are no morphological differences between Slovak and Hungarian samples. Because of this and considering the geographic and chronologic proximity between Rudabánya and Studienka A, our material is attributed to a similar, still unnamed form.

Discussion

Our study has yielded several new insights on the spatiotemporal distribution of late Miocene, central European Erinaceidae and Dimylidae. The late MN9 locality of Borský Svätý Jur evidences the first co-occurrence of *Lantanotherium sanmigueli* and '*Schizogalerix*' *voesendorfensis* (Table 4). The latter species is only identified in the MN7/8 and the earliest MN9 (e.g., Gratkorn, Felsőtárkány 2/3, Vösendorf), whereas *L. sanmigueli* is recorded during the MN9 in slightly younger localities (e.g., Can Ponsic I, Götzendorf, Rudabánya). This supports a late extinction of '*S.*' *voesendorfensis* in central Europe, after the apparent migration of *L. sanmigueli* from Asia (Cailleux et al., 2020). This also suggests that Borský Svätý Jur has an intermediate position between Vösendorf and Götzendorf, the former being the last occurence of *S. voesendorfensis* and the latter being the first occurence of *L. sanmigueli* in central Europe. Ziegler (2005b) described a small trigonid of a m3 (MAFI V20510) from Rudabánya (MN9), with a protolophid structure that could indicate a basal *Schizogalerix*. The co-occurrence of these two genera was also identified in the Ukrainian MN9 locality of Grytsiv, where *Schizogalerix* sp. indet. and *Lantanotherium* sp. indet. were recognized (Nesin and Kovalchuk, 2021). However, whereas '*S.*' *voesendorfensis* is found in western and central European localities during the MN9, eastern European localities were apparently occupied by another species, *S. sarmatica*.

The absence of *Plesiodimylus chantrei* at Borský Svätý Jur (Table 4) is surprising knowing its usual richness in deposits and its attested presence in the MN9 Austrian localities of the same basin (Ziegler, 2006b). The Dimylidae were otherwise extremely abundant during the Vallesian, representing > 30% of the Eulipotyphlan material in Studienka, Richardhof-Wald, and Schernham (Daxner-Höck et al., 2016, supplementary data). Their extremely fast decline during the earliest Turolian in the Pannonian region, as shown by the single element found from both Triblavina and Eichkogel, mirrors the overall rapid extinction of Dimylidae in the earliest Turolian.

The last occurrences of *Lantanotherium* in Europe are recorded during MN11, e.g., in Ambérieu 2 (Mein, 1999), Dorn-Dürkheim (Ziegler, 2006a), and possibly Csákvár under the name *Galerix hipparionum* Kretzoi, 1954 (see Kretzoi, 1954; Zijlstra and Flynn, 2015). Bachmayer and Wilson (1978) identified in the extremely rich locality of Kohfidisch (MN 11) a single lower molar of *Lantanotherium* that is here identified as a m3 of *L.* cf. *L. sanmigueli*. An inspection of the unpublished insectivore collection housed at NHMV revealed the presence of only one other specimen, a gracile, complete left M2 (Fig. 7.17; collection number 2021/0049/0001) also identified as *L.* cf. *L. sanmigueli*. On the other hand, the material from the MN11 of Krásno contains a high proportion of *L. sanmigueli*. This supports a slightly older age for Krásno or a spatial heterogeneity in the distribution of the last populations of *L. sanmigueli*. We noticed the presence of a single specimen of Dimylidae in Triblavina, but also in Eichkogel (Daxner-Höck et al., 2016, supplementary data), whereas the latter locality is considered slightly older than Kohfidisch and Krásno where dimylids are no longer recorded.

The material described here is characterized by a moderate diversity of erinaceids and dimylids in Slovakia, which was an expected result because central Europe is known as yielding a high overall diversity of insectivores (Furió et al., 2011; Van den Hoek Ostende et al., 2020). The Erinaceidae are dominated by the Galericinae, which are frequently encountered during the late Miocene. We observed the re-entrance of *Schizogalerix* in the Pannonian basin based on the MN11 fauna of Krásno and Eichkogel, leading to an increase in the regional abundance of Galericinae as noticed at Kohfidisch.

The history of *Schizogalerix* in the late Miocene of Europe can be split into two phases. The two MN9 species, '*Schizogalerix*' *voesendorfensis* and *S. sarmatica* are found in clearly separated regions, i.e., central Europe for '*S.*' *voesendorfensis* and eastern Europe for *S. sarmatica*. They share few morphological similarities because *S. sarmatica* is more advanced in the acquisition of the oblique dental pattern; they likely represent two different lineages. The Turolian is represented by *S. zapfei* and *S. moedligensis*, two species widely spread across Europe even if poorly recorded. *Schizogalerix moedlingensis* is found in Austria and Greece (Rabeder, 1973; Doukas et al., 1995) whereas *S. zapfei* is found in Austria and France (Bachmayer and Wilson, 1970; Mein, 1999). The northern Carpathians probably played a very minor role in this distribution because the reliefs surrounding the Danube and Vienna basins were still low. Both Turolian species share closer similarities in their morphological grade with *S. sarmatica* and likely belong to the same lineage. Thus, they could have an eastern European origin.

The diversity of central European Erinaceinae was low during the late Miocene. The few taxa (tentatively) identified in Austria and Slovakia are not significantly different from the few identified by Van Dam et al. (2020) in Spain. Moreover,

https://doi.org/10.1017/jpa.2023.50 Published online by Cambridge University Press

the highest diversity of Erinaceidae during the late Miocene of Slovakia is recorded in the MN11 of Krásno. A similar peak is observed in Spain during the MN11. This supports the suggestions of Van Dam et al. (2020) about a pan-European diversity phenomenon. Namely, the presence of few but widely spread species in Europe. Such a phenomenon seems to have persisted until the Pliocene before the entry of modern genera.

Conclusions

The collection of Eulipotyphla from the late Miocene of Slovakia indicates a moderate diversity but a high abundance of Erinaceidae and Dimylidae during the Vallesian. The material is dominated by '*Schizogalerix*' *voesendorfensis*. The occurrence of *S.* cf. *S. moedlingensis* in Krásno (MN11) supports the early Turolian re-emergence of *Schizogalerix* in central Europe, likely descending from a lineage that originated in eastern Europe. The dimylid *Plesiodimylus chantrei* is frequent in late MN9 and MN10 deposits. Rare specimens support its survival to early MN11. The marked decline in abundance of the erinaceids and dimylids between the Vallesian and the Turolian of Slovakia reflects a wider faunal and trophic turnover in eulipotyphlan fauna, coinciding with the regression of Lake Pannon.

Acknowledgments

We would like to thank J. van Dam, L. Voyta, editor J. Calede, and managing editor J. Kastigar for their valuable comments that significantly improved the manuscript. We are also very grateful to U.B. Göhlich, W. Wessels, and E. Robert for their kind help in providing comparative material from the paleontological collections in Vienna, Utrecht, and Lyon. This research was supported by the grants UK/27/2022 and UK/221/2023 from Comenius University, the Scientific Grant Agency of the Ministry of Education, Science, Research, and Sport of the Slovak Republic and Slovak Academy of Sciences (VEGA) under the contract VEGA 1/0533/21, the Slovak Research and Development Agency (project APVV-20-0120), and the Austrian Science Funds (FWF) under the project P-15724-N06.

Declaration of competing interests

The authors declare none.

Accessibility of supplemental data

Data available from the Dryad Digital Repository: https://doi.org/10.5061/dryad.79cnp5j1t.

References

Agustí, J., and Moyà-Solà, S., 1990, Mammal extinctions in the Vallesian (upper Miocene): Extinction Events in Earth History, v. 30, p. 425–432.

Anderson, J., 1895, On a new species of the genus *Erinaceus* from Somaliland: Proceedings of the Zoological Society, London, p. 414–421.

Andreae, A., 1904, Dritter beitrag zur binnen conchylien fauna des Miocäns von oppeln in schlesien: Mitteilungen Roemer-Museum Hildesheim, v. 20, p. 1–22.

Aymard, A., 1850, Compte rendu de la séance du 13 Avril 1849, réponse à M. Robert sur les mammifères fossiles des calcaires du Puy: Annales de la Société d'Agriculture du Puy, v. 14, p. 80–86.

Bachmayer, F., and Wilson, R.W., 1970, Die Fauna der altpliozänen Höhlen-und Spaltenfüllungen bei Kohfidisch, Burgenland (Österreich): small mammals (Insectivora, Chiroptera, Lagomorpha, Rodentia) from the Kohfidisch Fissures of Burgenland, Austria: Annalen des Naturhistorischen Museums in Wien, v. 74, p. 533–587.

Bachmayer, F., and Wilson, R.W., 1978, A second contribution to the fossil small mammal fauna of Kohfidisch, Austria: Annalen des Naturhistorischen Museums in Wien, v. 81, p. 129–161.

Bannikova, A.A., Lebedev, V.S., Abramov, A.V., and Rozhnov, V.V., 2014, Contrasting evolutionary history of hedgehogs and gymnures (Mammalia: Erinaceomorpha) as inferred from a multigene study: Biological Journal of the Linnean Society, v. 112, 499–519, https://doi.org/10.1111/bij.12299.

Baudelot, S., and Crouzel, F., 1976, Insectivore et lagomorphe à navère (lectoure) Burdigalien inférieur du Gers: Bulletin de la Société d'Histoire Naturelle de Toulouse, v. 112, p. 47–52.

Bi, S., Wu, W., Ye, J., and Meng, J., 1999, [Erinaceidae from the middle Miocene of north Junggar Basin, Xinjiang Uygur Autonomous Region, China], *in* Wang Yuanqing and Deng Tao, eds., Seventh Annual Meeting of the Chinese Society of Vertebrate Paleontology, Proceedings: Beijing, China Ocean Press, p. 157–165. (in Chinese)

Bolliger, T., 1992, *Kleinsäuger Stratigraphie in der miozänen Hörnli Schüttung (Ostschweiz) [Ph.D.* dissertation]: Zurich, Switzerland, ETH Zurich, 296 pp.

Butler, P.M., 1948, On the evolution of the skull and teeth in the Erinaceidae, with special reference to fossil material in the British Museum: Proceedings of the Zoological Society of London, v. 118, p. 446–500.

Cailleux, F., 2021, A spiny distribution: new data from Berg Aukas I (middle Miocene, Namibia) on the African dispersal of Erinaceidae (Eulipotyphla, Mammalia): Communications of the Geological Survey of Namibia, v. 23, p. 178–185.

Cailleux, F., Chaimanee, Y., Jaeger, J.-J., and Chavasseau, O., 2020, New Erinaceidae (Eulipotyphla, Mammalia) from the middle Miocene of Mae Moh, northern Thailand: Journal of Vertebrate Paleontology. v. 40, n. e1783277, https://doi.org/10.1080/02724634.2020.1783277.

Crespo, V.D., Furió, F., Ruiz-Sánchez, F.J., and Montoya, P., 2018, A new species of *Plesiodimylus* (Dimylidae, Eulipotyphla, Mammalia) from the early Miocene of Spain: Historical Biology, v. 30, p. 360–371, https://doi.org/10.1080/08912963.2017.1289519.

Crespo, V.D., Sevilla, P., Montoya, P., and Ruiz-Sanchez, F.J., 2020, A relict tropical forest bat assemblage from the early Miocene of the Ribesalbes-Alcora Basin (Castelló, Spain): Earth and Environmental Science Transactions of the Royal Society of Edinburgh, v. 111, p. 247–258, https://doi.org/10.1017/S1755691020000122.

Crusafont, M., and Villalta, J.F., 1947, Sur un *Palerinaceus* du Pontien d'Espagne: Eclogae Geologicae Helvetiae, v. 40, p. 320–333.

Crusafont-Pairó, M., and Golpe, J.M., 1972, Dos nuevos yacimientos del Vindoboniense en el Vallés: Acta Geologica Hispanica, v. 7, p. 71–72.

Daxner-Höck, G., Harzhauser, M., and Göhlich, U.B., 2016, Fossil record and dynamics of late Miocene small mammal faunas of the Vienna Basin and adjacent basins, Austria: Comptes Rendus Palevol, v. 15, p. 855–862, https://doi.org/10.1016/J.CRPV.2015.06.008.

De Bruijn, H., Mayda, S., Van den Hoek Ostende, L.W., Kaya, T., and Saraç, G., 2006, Small mammals from the early Miocene of Sabuncubeli (Manisa, SW Anatolia, Turkey): Beiträge zur Paläontologie, v. 30, p. 57–87.

Doukas, C.S., 1986, The mammals from the lower Miocene of Aliveri (island of Evia, Greece): Proceedings of the Koninklijke Nederlandse Akademie van Wetenschappen B, v. 89, p. 15–38.

Doukas, C.S., van den Hoek Ostende, L.W., Theocharopoulos, C., and Reumer, J.W.F., 1995, Insectivora (Erinaceidae, Talpidae, Soricidae, Mammalia), *in* Schmidt-Kittler, N., ed., The Vertebrate Locality Maramena (Macedonia, Greece) at the Turolian-Ruscinian Boundary: Münchner Geowissenschaftliche Abhandlungen, v. A28, p. 43–64.

Duvernoy, G.L., and Lereboullet, A., 1842, Notes et renseignements sur les animaux vertébrés de l'Algérie qui font partie du musée de Strasbourg, *in* Levrault, F.G. (publisher), Mémoire de la Société d'Histoire Naturelle de Strasbourg, v. 3, 1840–1846, p. 260–351.

Engesser, B., 1972, Die obermiozäne säugetierfauna von Anwil (Baselland) [Inaugural dissertation]: Liestal, Switzerland, Lüdin AG, 363 pp.

Engesser, B., 1980, Relationships of some insectivores and rodents from the Miocene of North America and Europe: Bulletin of the Carnegie Museum of Natural History, v. 14, p. 1–68.

Engesser, B., 2009, The insectivores (Mammalia) from Sansan (middle Miocene, south-western France): Schweizerische Paläontologische Abhandlungen, v. 128, p. 1–91.

Engesser, B., and Jiang, X.-L., 2011, Odontological and craniological comparisons of the Recent hedgehog *Neotetracus* with *Hylomys* and *Neohylomys* (Erinaceidae, Insectivora, Mammalia): Vertebrata PalAsiatica, v. 49, p. 406–422.

Fahlbusch, V., 1989, Über den Holotypus von *Metacordylodon schlosseri* (Andreae 1904) (Insectivora, Mamm.) aus dem Miozän von Opole

(Oppeln): Mitteilungen der Bayerischen Staatssammlung für Paläontologie und Historische Geologie, v. 29, p. 159–162.
Fejfar, O., and Sabol, M., 2005, Czech Republic and Slovak Republic, *in* Van den Hoek Ostende, L.W., Doukas, C.S., and Reumer, J.W.F., eds., The Fossil Record of the Eurasian Neogene Insectivores (Erinaceomorpha, Soricomorpha, Mammalia), Part I: Scripta Geologica Special Issue, v. 5, p. 51–60.
Fejfar, O., and Sabol, M., 2009, Middle Miocene *Plesiodimylus* from the Devínska Nová Ves-Fissures site (western Slovakia): Bulletin of Geoscience, v. 84, p. 611–624, https://doi.org/10.3140/bull.geosci.1148.
Filhol, H., 1888, Sur un nouveau genre d'insectivore: Bulletin de la Société Phylomatique de Paris, v. 7, p. 24–25.
Fischer, G., 1814, Zoognosia Tabulis Synopticis Illustrata, Volumen Tertium: Quadrupedum Reliquorum, Cetorum et Monotrymatum Descriptionem Continens: Moscow, Nicolai Sergeidis Vsevolozsky, 732 p.
Frost, D.R., Wozencraft, W.C., and Hoffmann, R.S., 1991, Phylogenetic relationships of hedgehogs and gymnures (Mammalia: Insectivora: Erinaceidae): Smithsonian Contributions to Zoology, v. 518, p. 1–69.
Furió, M., and Agustí, J., 2017, Latest Miocene insectivores from eastern Spain: Evidence for enhanced latitudinal differences during the Messinian: Geobios, v. 50, p. 123–140, https://doi.org/10.1016/j.geobios.2017.02.001.
Furió, M., and Alba, D., 2011, Aspectos problemáticos del género *Lantanotherium* (Galericinae, Erinaceidae, Mammalia), *in* Pérez-García, A., Gascó, F., Gasulla, J.M., and Escaso, F., eds., Viajando a Mundos Pretéritos: Madrid, Ayuntamiento de Morella, p. 123–130.
Furió, M., Alba, D., Carmona, R., and Rifà, E., 2011a, New fossil remains of *Lantanotherium* (Erinaceidae, Mammalia) from the Vallesian (late Miocene) of Viladecavalls (NE Spain): 71st Annual Meeting Society of Vertebrate Paleontology, Las Vegas, Nevada, USA, Program and Abstracts, supplement to online Journal of Vertebrate Paleontology, p. 113.
Furió, M., Casanovas-Vilar, I., and Van Den Hoek Ostende, L.W., 2011b, Predictable structure of Miocene insectivore (Lipotyphla) faunas in western Europe along a latitudinal gradient: Palaeogeography, Palaeoclimatology, Palaeoecology, v. 304, p. 219–229, https://doi.org/10.1016/j.palaeo.2010.01.039.
Furió, M., Van den Hoek Ostende, L.W., Agustí, J., and Minwer-Barakat, R., 2017, Evolución de las asociaciones de insectívoros (Eulipotyphla, Mammalia) en España y su relación con los cambios climáticos del Neógeno y el Cuaternario: Ecosistemas, v. 27, p. 38–51, https://doi.org/10.7818/ECOS.1454.
Gaillard, C., 1897, Nouveau genre d'insectivores du Miocène moyen de la Grive-Saint-Alban (Isère): Comptes Rendus Hebdomadaires des Séances de l'Académie des Sciences, v. 124, p. 1248–1250.
Gaillard, C., 1899, Mammifères Miocènes nouveaux ou peu connus de La Grive-Saint-Alban (Isère) : Archives du Muséum d'Histoire Naturelle de Lyon, v. 7, p. 1–79.
Gibert, J., 1975, New insectivores from the Miocene of Spain: Proceedings of the Koninklijke Nederlandse Akademie van Wetenschappen, v. 78, p. 108–133.
Gould, G.C., 2001, The phylogenetic resolving power of discrete dental morphology among extant hedgehogs and the implications for their fossil record: American Museum Novitates, v. 2001, p. 1–52, https://doi.org/10.1206/0003-0082(2001)340<0001:TPRPOD>2.0.CO;2.
Harzhauser, M., and Mandič, O., 2008, Neogene lake systems of central and south-eastern Europe: faunal diversity, gradients and interrelations: Palaeogeography, Palaeoclimatology, Palaeoecology, v. 260, p. 417–434, https://doi.org/10.1016/j.palaeo.2007.12.013.
Hír, J., Venczel, M., Codrea, V., Angelone, C., Van den Hoek Ostende, L.W., Kirscher, U., and Prieto, J., 2016, Badenian and Sarmatian s. str. from the Carpathian area: overview and ongoing research on Hungarian and Romanian small vertebrate evolution: Comptes Rendus Palevol, v. 15, p. 863–875, https://doi.org/10.1016/j.crpv.2016.08.001.
Hír, J., Venczel, M., Codrea, V., Rossner, G.E., Angelone, C., Van den Hoek Ostende, L.W., Rosina, V.V., Kirscher, U., and Prieto, J., 2017, Badenian and Sarmatian s. str. from the Carpathian area: taxonomical notes concerning the Hungarian and Romanian small vertebrates and report on the ruminants from the Felsőtárkány Basin: Comptes Rendus Palevol, v. 16, p. 312–332, https://doi.org/10.1016/j.crpv.2016.08.001.
Jablonski, N.G., Su, D.F., Flynn, L.J., Ji, X., Deng, C., et al., 2014, The site of Shuitangba (Yunnan, China) preserves a unique, terminal Miocene fauna: Journal of Vertebrate Paleontology, v. 34, p. 1251–1257, https://doi.org/10.1080/02724634.2014.843540.
James, G.T., 1963, Paleontology and nonmarine stratigraphy of the Cuyama Valley badlands, California, part 1, geology, faunal interpretations, and systematic descriptions of Chiroptera, Insectivora, and Rodentia: University of California Publications in Geological Sciences, v. 45, p. 1–154.
Jenkins, P. D., and Robinson, M. F., 2002, Another variation on the gymnure theme: description of a new species of *Hylomys* (Lipotyphla, Erinaceidae, Galericinae): Bulletin of the Natural History Museum, London, Zoology Series, v. 68, p. 1–11, https://doi.org/10.1017/S0968047002000018.
Joniak, P., 2005, New rodent assemblages from the upper Miocene deposits of the Vienna Basin and Danube Basin [Thesis]: Bratislava, Slovakia, Comenius University, 126 p..
Joniak, P., 2016, Upper Miocene rodents from Pezinok in the Danube Basin, Slovakia: AGEOS (Acta Geologica Slovaca), v. 8, p. 1–14.
Joniak, P., and Šujan, M., 2020, Systematic and morphometric data of late Miocene rodent assemblage from Triblavina (Danube Basin, Slovakia): Data in Brief, v. 28, n. e104961, https://doi.org/10.1016/j.dib.2019.104961.
Joniak, P., Šujan, M., Fordinál, K., Braucher, R., Rybár, S., Kováčová, M., Kováč, M., and Aster Team, 2020, The age and paleoenvironment of a late Miocene floodplain alongside Lake Pannon: rodent and mollusk biostratigraphy coupled with authigenic $^{10}Be/^{9}Be$ dating in the northern Danube Basin of Slovakia: Palaeogeography, Palaeoclimatology, Palaeoecology, v. 538, n. 109482, https://doi.org/10.1016/j.palaeo.2019.109482.
Kälin, D., and Engesser, B., 2001, Die jungmiozäne Säugetierfauna vom Nebelbergweg bei Nünningen (Kanton Solothurn, Schweiz): Schweizerische Paläontologische Abhandlungen, v. 121, p. 1–6.
Klietmann, J., 2013, Systematic and ecological analysis of Marsupialia and Eulipotyphla from Petersbuch 28 (Germany, lower Miocene) [Ph.D. Thesis]: Vienna, Austria, University of Vienna, 484 p.
Klietmann, J., Nagel, D., Rummel, M., and Van den Hoek Ostende, L.W., 2014a, *Amphiperatherium* and Erinaceidae of Petersbuch 28: Bulletin of Geosciences, v. 89, p. 1–20, https://doi.org/10.3140/bull.geosci.1454.
Klietmann, J., Nagel, D., Rummel, M., and van den Hoek Ostende, L.W., 2014b, Enlightening complexity: the Dimylidae of Petersbuch 28: Palaeobiodiversity and Palaeoenvironments, v. 94, p. 463–479, https://doi.org/10.1007/s12549-013-0137-5.
Klietmann, J., van den Hoek Ostende, L.W., Nagel, D., and Rummel, M., 2015, Insectivore palaeoecology: a case study of a Miocene fissure filling in Germany: Palaeogeography, Palaeoclimatology, Palaeoecology, v. 418, p. 278–289, https://doi.org/10.1016/j.palaeo.2014.11.019.
Korth, W.W., and Evander, R.L., 2016, Lipotyphla, Chiroptera, Lagomorpha, and Rodentia (Mammalia) from Observation Quarry, earliest Barstovian (Miocene), Dawes County, Nebraska: Annals of Carnegie Museum, v. 83, p. 219–254, https://doi.org/10.2992/007.083.0301.
Kováč, M., Synak, R., Fordinal, K., Joniak, P., Toth, C., et al., 2011, Late Miocene and Pliocene history of the Danube Basin: inferred from development of depositional systems and timing of sedimentary facies changes: Geologica Carpathica, v. 62, p. 519–534, https://doi.org/10.2478/v10096-011-0037-4.
Kováč, M., Márton, E., Oszczypko, N., Vojtko, R., Hok, J., et al., 2017, Neogene palaeogeography and basin evolution of the Western Carpathians, northern Pannonian domain and adjoining areas: Global and Planetary Change, v. 155, p. 133–154, https://doi.org/10.1016/j.gloplacha.2017.07.004.
Kretzoi, M., 1954, Befejező jelentés a Csákvári barlang őslenytani feltárásáról: MÁFI Évi Jelentése az 1952, Évről, p. 37–69.
Lartet, E., 1851, Notice sur la colline de Sansan: Annuaire du Département du Gers, 42 p.
Li, Z., Li, Y., Xue, X., Li, W., Zhang, Y., and Yang, F., 2019, A new fossil Erinaceidae from the Shajingyi area in the Lanzhou Basin, China: Acta Geologica Sinica (English Edition), v. 93, p. 789–798, https://doi.org/10.1111/1755-6724.13797.
Linnaeus, C., 1758, Systema Naturae per Regna Tria Naturae (tenth edition), Volume 1, Regnum Animale: Stockholm, Laurentii Salvii, 824 p.
Lungu, A.N., 1981, [The Hipparion fauna of the Middle Sarmatian of Moldavia (Insectivora, Lagomorpha, Rodentia)]: Kishinev, Moldova, Shtiintsa, 140 p. [in Russian]
Magyar, I., Geary, D.H., and Müller, P., 1999, Paleogeographic evolution of the late Miocene Lake Pannon in central Europe: Palaeogeography, Palaeoclimatology, Palaeoecology, v. 147, p. 151–167.
Magyar, I., Radivojević, D., Sztanó, O., Synak, R., Ujszászi, K., and Pócsik, M., 2013, Progradation of the paleo-Danube shelf margin across the Pannonian Basin during the late Miocene and early Pliocene: Global and Planetary Change, v. 103, p. 168–173, https://doi.org/10.1016/j.gloplacha.2012.06.007.
Mein, P., 1999, The late Miocene small mammal succession from France, with emphasis on the Rhône Valley localities, *in* Agustí, J., Rook, L., and Andrews, P., eds., Hominoid Evolution and Climatic Change in Europe, 1: Cambridge, U.K., Cambridge University Press, p. 140–164.
Mein, P., and Ginsburg, L., 1997, Les mammifères du gisement Miocène inférieur de Li Mae Long, Thaïlande: systématique, biostratigraphie et paléoenvironnement: Geodiversitas, v. 19, p. 783–844.
Mein, P., and Ginsburg, L., 2002, Sur l'âge relatif des différents dépôts karstiques Miocènes de La Grive-Saint-Alban (Isère): Cahiers Scientifiques du Muséum d'Histoire Naturelle de Lyon, Centre de Conservation et d'Étude des Collections, v. 5, p. 7–47, https://doi.org/10.3406/mhnly.2002.1328.
Mein, P., and Martin-Suárez, E.M., 1993, *Galerix iberica* sp. nov. (Erinaceidae, Insectivora, Mammalia) from the late Miocene and early Pliocene of the Iberian Peninsula: Geobios, v. 26, p. 723–730.

Mein, P., Moissenet, E., and Adrover, R., 1990, Biostratigraphie du Neogene superieur du bassin de Teruel: Paleontologia i Evolucion, v. 23, p. 121–139.
Ménouret, B., and Mein, P., 2008, Les vertébrés du Miocène supérieur de Soblay (Ain, France): Travaux et Documents des Laboratoires de Géologie de Lyon, no. 165, 97 p.
Meyer, C.E.H., Von, 1865, Briefe an den Herausgeber: Neues Jahrbuch für Mineralogie, Geologie und Paläontologie, p. 215–221.
Müller, A., 1967, Die Geschichte der Familie Dimylidae (Insectivora, Mamm.) auf Grund der Funde aus tertiären Spaltenfüllungen Süddeutschlands [Ph.D. dissertation]: München, Germany, ayerische Akademie der Wissenschaften, 93 p.
Nesin, V.A., and Kovalchuk, O., 2021, A new late Miocene *Anomalomys* species from western Ukraine with implications for the diversity and evolution of anomalomyid rodents in eastern Europe: Historical Biology, v. 33, p. 1809–1816, https://doi.org/10.1080/08912963.2020.1742711.
Pomel, N.A., 1848, Études sur les carnassiers insectivores, 1: insectivores fossiles, 2: classification des insectivores: Archives des Sciences Physiques et Naturelles, v. 9, p. 159–165, 244–251.
Prieto, J., and Rummel, M., 2009, Erinaceidae (Mammalia, Erinaceomorpha) from the middle Miocene fissure filling Petersbuch 68 (southern Germany): Zitteliana, v. 48/49, p. 75–88.
Prieto, J., Gross, M., Böhmer, C., and Böhme, M., 2010, Insectivores and bat (Mammalia) from the late middle Miocene of Gratkorn (Austria): biostratigraphic and ecologic implications: Neues Jahrbuch für Geologie und Paläontologie Abhandlungen, v. 258, p. 107–119, https://doi.org/10.1127/0077-7749/2010/0088.
Prieto, J., Angelone, C., Casanovas-Vilar, I., Gross, M., Hír, J., Van den Hoek Ostende, L.W., Maul, L.C., and Vasilyan, D., 2014, The small mammals from Gratkorn: an overview: Palaeobiodiversity and Palaeoenvironments, v. 94, p. 135–162, https://doi.org/10.1007/s12549-013-0147-3.
Qiu, Z.D., 1996, Middle Miocene Micromammalian Fauna from Tunggur, Inner Mongolia: Beijing, Science Press, 216 p.
Rabeder, G., 1973, *Galerix* und *Lanthanotherium* (Erinaceidae, Insectivora) aus dem Pannon des Wiener Beckens: Neues Jahrbuch für Geologie und Paläontologie Monatshefte, v. 7, p. 429–446.
Rzebik-Kowalska, B., 1996, Insectivora (Mammalia) from the Miocene of Bełchatów, Poland, 3, Dimylidae Schlosser, 1887: Acta Zoologica Cracova, v. 39, p. 447–468.
Rzebik-Kowalska, B., and Lungu, A., 2009, Insectivore mammals from the late Miocene of the Republic of Moldova: Acta Zoologica Cracoviensia, Series A, Vertebrata, v. 52, p. 11–60, https://doi.org/10.3409/azc.52a_1-2.11-60.
Sabol, M., Joniak., P., Bilgin, M., Bonilla-Salomón, I., Cailleux, F., Čerňanský, A., Malíková, V., Šedivá, M., and Tóth, C., 2021, Updated Miocene mammal biochronology of Slovakia: Geologica Carpathica, v. 72, p. 425–443, https://doi.org/10.31577/GeolCarp.72.5.5.
Schlosser, M., 1887, Die Affen, Lemuren, Chiropteren, Insectivoren, Marsupialier, Creodonten und Carnivoren des Europaischen Tertiars und deren Beziehungen zu ihren lebenden und fossilen aussereuropaischen Verwandten, Theil 1: Beiträge zur Paläontologie Österreich-Ungarns und des Orients, Wien, v. 6, 244 p., 9 pls.
Schlosser, M., 1911, Beitrage zur Kenntnis der oligozanen Landsaugetiere aus dem Fayum, Agypten: Beitrage zur Palaontologie und Geologie Osterreich-Ungarns, v. 24, p. 1–167.
Schötz, M., 1985, Die Dimyliden (Mammalia, Insectivora) aus dem Kiesgrube Niederaichbach und Maßendorf (Obere Süßwassermolasse Niederbayerns): Mitteilungen der Bayerischen Staatssammlung für Paläontologie und Historische Geologie, v. 25, p. 95–130.
Seemann, I., 1938, Die Insektenfresser, Fledermäuse und Nager aus der obermiocänen Braunkohle von Viehhausen bei Regensburg: Palaeontographica Abteilung A, v. 1–3, p. 1–56.
Selänne, L., 2003, Genus *Schizogalerix* (Insectivora), *in* Fortelius, M., Kappelman, J., Sen, S., and Bernor, R.L., eds., Geology and Paleontology of the Miocene Sinap Formation, Turkey: New York, Colombia University Press, p. 69–89.
Sen, S., 1990, Stratigraphie, faunes de mammifères et magnétostratigraphie du Néogène de Sinap Tepe, Province d'Ankara, Turquie: Bulletin du Muséum National d'Histoire Naturelle: Sciences de la Terre, Paléontologie, Géologie, Minéralogie, Section C, v. 12, p. 243–277.
Shaw, T.H., and Wong S., 1959, [A new insectivore from Hainan]: Acta Zoologica Sinica, v. 11, p. 422–425. (in Chinese)
Smith, A., 1831, Contributions to the natural history of South Africa, No. 1: South African Quarterly Journal, ser. 1, v. 1, p. 9–24.
Storch, G., and Qiu, S., 1991, Insectivores (Mammalia: Erinaceidae, Soricidae, Talpidae) from the Lufeng hominoid locality, late Miocene of China: Geobios, v. 24, p. 601–621.
Šujan, M., Braucher, R., Kováč, M., Bourlčs, D.L., Rybár, S., Guillou, V., and Hudáčková, N., 2016, Application of the authigenic $^{10}Be/^{9}Be$ dating method to late Miocene–Pliocene sequences in the northern Danube Basin (Pannonian Basin System): confirmation of heterochronous evolution of sedimentary environments: Global and Planetary Change, v. 137, p. 35–53, https://doi.org/10.1016/j.gloplacha.2015.12.013.
Sulimski, A., 1959, Insectivores du Pliocène de Węże: Acta Palaeontologica Polonica, v. 4, p. 119–179.
Thenius, E., 1949, Zur Revision der Insektivoren des steirischen Tertiärs Beiträge zur Kenntnis der Säugetierreste des steirischen Tertiärs, 2: Paläontologisches und Paläobiologisches Institut der Universität, v. 1, p. 671–693.
Trouessart, E.-L., 1909, *Neotetracus sinensis*, a new insectivore of the family Erinaceidae: Annals and Magazine of Natural History, v. 4, p. 389–391.
Utescher, T., Erdei, B., Hably, L., and Mosbrugger, V., 2017, Late Miocene vegetation of the Pannonian Basin: Palaeogeography, Palaeoclimatology, Palaeoecology, v. 467, p. 131–148, https://doi.org/10.1016/j.palaeo.2016.02.042.
Van Dam, J.A., 2004, Anourosoricini (Mammalia: Soricidae) from the Mediterranean region: a pre-Quaternary example of recurrent climate-controlled north-south range shifting: Journal of Paleontology, v. 78, p. 741–764, https://doi.org/10.1666/0022-3360(2004)078<0741:AMSFTM>2.0.CO;2.
Van Dam, J.A., 2006, Geographic and temporal patterns in the late Neogene (12–3 Ma) aridification of Europe: the use of small mammals as paleoprecipitation proxies: Palaeogeography, Palaeoclimatology, Palaeoecology, v. 238, p. 190–218, https://doi.org/10.1016/j.palaeo.2006.03.025.
Van Dam, J.A., Mein, P., and Alcalá, L., 2020, Late Miocene Erinaceinae from the Teruel Basin (Spain): Geobios, v. 61, p. 61–81, https://doi.org/10.1016/j.geobios.2020.06.002.
Van Dam, J.A., Mein, P., Garcés, M., van Balen, R.T., Furió, M., and Alcalá, L., 2023, A new rodent chronology for the late Neogene of Spain: Geobios, v. 76, p. 53–74, https://doi.org/10.1016/j.geobios.2023.01.001.
Van den Hoek Ostende, L.W., 2001, A revised generic classification of the Galericini (Insectivora, Mammalia) with some remarks on their palaeobiogeography and phylogeny: Geobios, v. 34, p. 681–695, https://doi.org/10.1016/S0016-6995(01)80029-2.
Van den Hoek Ostende, L.W., and Fejfar, O., 2015, All time high: Dimylidae (Eulipotyphla, Mammalia) diversity in the early Miocene locality of Ahníkov 1 (Czech Republic, MN 3): Palaeobiodiversity and Palaeoenvironments, v. 95, p. 453–464, https://doi.org/10.1007/s12549-015-0210-3.
Van den Hoek Ostende, L.W., Furió, M., Madern, A., and Prieto, J., 2016, Enters the shrew, some considerations on the Miocene palaeobiogeography of Iberian insectivores: Comptes Rendus Palevol, v. 15, p. 813–823, https://doi.org/10.1016/j.crpv.2016.03.006.
Van den Hoek Ostende, L.W., Bilgin, M., Braumuller, Y., Hír, Y., Joniak, P., et al., 2020, Generically speaking, a survey on Neogene rodent diversity at the genus level in the NOW database: Fossil Imprint, v. 76, p. 118–127, https://doi.org/10.37520/fi.2020.008.
Van den Hoek Ostende, L.W., Bilgin, M., Braumuller, Y., Cailleux, F., and Skandalos, P., 2023, Live long and prosper? Assessing longevity of small mammal taxa using the NOW database, *in* Casanovas-Vilar, I., van den Hoek Ostende, L.W., Janis, C.M., and Saarinen, J., eds., Evolution of Cenozoic Land Mammal Faunas and Ecosystems: 25 Years of the NOW Database of Fossil Mammals, Vertebrate Paleobiology and Paleoanthropology: Cham, Switzerland, Springer International Publishing, p. 111–129.
Van der Made, J., Morales, J., and Montoya, P., 2006, Late Miocene turnover in the Spanish mammal record in relation to paleoclimate and the Messinian Salinity Crisis: Palaeogeography, Palaeoclimatology, Palaeoecology, v. 238, p. 228–246, https://doi.org/10.1016/j.palaeo.2006.03.030.
Vasileiadou, K., and Doukas, C.S., 2021, The fossil record of insectivores (Mammalia: Eulipotyphla) in Greece, *in* Vlachos, E., ed., Fossil Vertebrates of Greece, Volume 2: Cham, Switzerland, Springer, p. 33–92.
Villalta, J.F., and Crusafont, M., 1944, Nuevos insectívoros del Mioceno continental del Vallés-Penedés: Notas y Comunicaciones del Instituto Geológico y Minero de España, v. 12, p. 39–65.
Viret, J., 1931, Découverte de *Metacordylodon schlosseri* à La-Grive-Saint-Alban: Bulletin de la Société d'Histoire Naturelle de Toulouse, v. 61, p. 253–257.
Viret, J., 1938, Étude sur quelques erinacéidés fossiles spécialement sur le genre *Palaerinaceus*: Travaux du Laboratoire de Géologie de la Faculté des Sciences de Lyon, Mémoires, v. 28, p. 1–35.
Viret, J., 1940, Etude sur quelques érinacéidés fossiles (suite): genres *Plesiosorex, Lanthanotherium*: Travaux du Laboratoire de Géologie de la Faculté des Sciences de Lyon, Mémoires, v. 39, p. 33–65.
Voyta, L.L., 2017, Age related cranial characters from the viewpoint of species identification of Amur and Daurian hedgehogs (Lipotyphla: Erinaceidae): Russian Journal of Theriology, v. 16, p. 176–184, https://doi.org/10.15298/rusjtheriol.16.2.06.
Waddell, P.J., Okada, N., and Hasegawa, M., 1999, Towards resolving the interordinal relationships of placental mammals: Systematic Biology, v. 48, p. 1–5.
Wagner, J.A., 1841, Die Raubthiere, *in* Schreber, J.C.D., Goldfuss, G.A., and Wagner, J.A., eds., Die Säugthiere in Abbildungen nach der Natur, Suppl. Abt. 2: Leipzig, Germany, 810 p.

https://doi.org/10.1017/jpa.2023.50 Published online by Cambridge University Press

Wegner, R.N., 1913, Tertiär umgelagerte Kreide bei Oppeln (Oberschlesien): Palaeontographica, Beitraege zur Naturgeschichtie der Vorzeit, v. 60, p. 175–274.

Ziegler, R., 1983, *Odontologische und osteologische Untersuchungen an* Galerix exilis *(Blainville) (Mammalia, Erinaceidae) aus den miozänen Ablagerungen von Steinberg und Goldberg im Nördlinger Ries (Süddeutschland)* [Ph.D. dissertation]: München, Germany, Ludwig Maximilian University, 277 pp.

Ziegler, R., 2000, The Miocene Fossil-Lagerstätte Sandelzhausen, 17, Marsupialia, Lipotyphla and Chiroptera (Mammalia): Senckenbergiana Lethaea, v. 80, p. 81–127, https://doi.org/10.1007/BF03043666.

Ziegler, R., 2005a, Erinaceidae and Dimylidae (Lipotyphla) from the upper middle Miocene of South Germany: Senckenbergiana Lethaea, v. 85, p. 131–152, https://doi.org/10.1007/BF03043423.

Ziegler, R., 2005b, The insectivores (Erinaceomorpha and Soricomorpha, Mammalia) from the late Miocene hominoid locality Rudabánya: Palaeontographia Italica, v. 90, p. 53–81.

Ziegler, R., 2006b, Insectivores (Lipotyphla) and bats (Chiroptera) from the late Miocene of Austria: Annalen des Naturhistorischen Museums in Wien, Serie A, Für Mineralogie und Petrographie, Geologie und Paläontologie, Anthropologie und Prähistorie, v. 1, p. 93–196.

Ziegler, R., 2006a, Miocene Insectivores from Austria and Germany–an overview: Beiträge zur Paläontologie, v. 30, p. 481–494.

Zijlstra, J., and Flynn, L.J., 2015, Hedgehogs (Erinaceidae, Lipotyphla) from the Miocene of Pakistan, with description of a new species of *Galerix*: Palaeobiodiversity and Palaeoenvironments, v. 95, p. 477–495, https://doi.org/10.1007/s12549-015-0190-3.

Zouhri, S., Benammi, M., Geraads, D., and El Boughabi, S., 2017, Mammifères du Néogène continental du Maroc: faunes, biochronologie et paléobiogéographie: Mémoires de la Société Géologique de France, v. 180, p. 527–588.

Accepted: 8 August 2023